




RESEARCH ARTICLE

Towards recognizing the mechanisms of effects evoked in living organisms by static magnetic field. Numerically simulated effects of the static magnetic field upon simple inorganic molecules. [version 1; peer review: awaiting peer review]

Wojciech Ciesielski ¹, Tomasz Girek¹, Zdzisław Oszczęda², Jacek Soroka³, Piotr Tomasik²

¹Institute of Chemistry, Jan Długosz University, Częstochowa, 42-201, Poland

²Nantes Nanotechnological Systems, Bolesławiec, 59700, Poland

³Scientific Society of Szczecin, Szczecin, 71-481, Poland

V1 First published: 20 Jul 2021, 10:611
<https://doi.org/10.12688/f1000research.54436.1>
Latest published: 20 Jul 2021, 10:611
<https://doi.org/10.12688/f1000research.54436.1>

Abstract

Background: Recognizing effects of static magnetic field (SMF) of varying flux density on flora and fauna is attempted. For this purpose, the influence of static magnetic field upon molecules of water, nitrogen, ammonia, carbon dioxide, methane and molecular oxygen was studied.

Methods: Computations of the effect of SMF of 0.1, 1, 10 and 100T flux density were performed in a computer vacuum involving advanced computational methods.

Results: It was shown that SMF polarizes molecules depending on applied flux density but it neither ionizes nor breaks valence bonds. Three-molecular conglomerates of very dense packing form systems involving supramolecular orbitals. These orbitals deteriorate with an increase in the SMF flux density developing highly polarized structures. They are entirely different from these originally formed out of SMF.

Conclusions: Small inorganic molecules commonly present in living organisms of flora and fauna can substantially influence functioning of those organisms when exposed to SMF.

Keywords

ammonia, carbon dioxide, methane, nitrogen, organisms, oxygen, static magnetic field, water

Open Peer Review

Reviewer Status AWAITING PEER REVIEW

Any reports and responses or comments on the article can be found at the end of the article.

Corresponding author: Wojciech Ciesielski (w.ciesielski@interia.pl)

Author roles: **Ciesielski W:** Conceptualization, Investigation, Methodology, Software, Visualization; **Girek T:** Investigation, Validation; **Oszczęda Z:** Visualization; **Soroka J:** Supervision, Validation, Writing – Review & Editing; **Tomasik P:** Conceptualization, Formal Analysis, Methodology, Supervision, Writing – Original Draft Preparation, Writing – Review & Editing

Competing interests: No competing interests were disclosed.

Grant information: The author(s) declared that no grants were involved in supporting this work.

Copyright: © 2021 Ciesielski W *et al.* This is an open access article distributed under the terms of the [Creative Commons Attribution License](#), which permits unrestricted use, distribution, and reproduction in any medium, provided the original work is properly cited.

How to cite this article: Ciesielski W, Girek T, Oszczęda Z *et al.* **Towards recognizing the mechanisms of effects evoked in living organisms by static magnetic field. Numerically simulated effects of the static magnetic field upon simple inorganic molecules.** [version 1; peer review: awaiting peer review] F1000Research 2021, 10:611 <https://doi.org/10.12688/f1000research.54436.1>

First published: 20 Jul 2021, 10:611 <https://doi.org/10.12688/f1000research.54436.1>

Introduction

There are a considerable number of monographs¹⁻³ and papers⁴⁻¹² characterizing the effects of all kinds of magnetic field upon flora and fauna. Currently, a focus is noted on the effect of magnetic resonance imaging on humans¹³⁻¹⁶. There are several reports with well documented biological effects of magnetic field. However, their interpretation and considerations on mechanisms of those effects on the molecular level are scarce¹⁶⁻²⁰. Because of increasing environmental pollution with magnetic fields^{21,22} and considerable involvement of magnetic fields in current and future technologies²³⁻²⁵ this problem should attract particular attention.

Recently, Jaworska *et al.*, reported the stimulating effect of water treated with static magnetic field (SMF) of up to ~0.2T upon the growth and pathogenicity of entomopathogenic organisms both nematodes²⁶ and fungi^{27,28}. These results suggested a modification of the water macrostructure. Thus, one might assume that SMF can influence hydration of biological membranes and objects within the living cells. Turning the water macrostructure into smaller clusters^{29,30} could facilitate the penetration of water across membranes into the cells. Also structures of nitrogen, ammonia and carbon dioxide molecules present in living organisms could be modified by SMF and these processes might be involved in the observed effects. Białopiotrowicz *et al.*²⁹ reported formation of singlet oxygen on a treatment of water saturated with air with a low-temperature, low-pressure glow plasma of low frequency. The singlet oxygen molecules were stabilized by their incorporation into aqueous clathrates of the nanometric dimensions.

These factors strongly suggested that water and small inorganic molecules could participate in the observed effects of magnetic field and control mechanisms and kinetics of phenomena induced by SMF.

This paper presents results of computational simulations of the structure of molecular oxygen, nitrogen, water, carbon dioxide, ammonia and methane in SMF of the flux density from 0 to 100T.

Methods

Numerical computations

Molecular structures were drawn using the Fujitsu SCIGRESS 2.0 software³¹ (open-access alternative software: [GaussView 6](#)). Their principal symmetry axes were oriented along the x-axis of the Cartesian system. The magnetic field was fixed in the same direction with the south pole from the left side. Subsequently, the molecules were optimized involving Gaussian 0.9 software equipped with the 6-31G** basis³² (open-access alternative software: [Spartan 1.0.0](#)). For those optimized single molecules bond lengths, dipole moments, heats of formation and bond energies were computed. Additionally, computations of HOMO/LUMO energy level for single molecules as well as HOMO/LUMO energy level and total energy for systems built of three molecules were also performed.

In the consecutive step, influence of SMF upon optimized molecules were computed with Amsterdam Modeling Suite software^{33,34} (open-access alternative software: [ORCA 5.0](#)), and the NR_LDOTB (non-relativistically orbital momentum L-dot-B) method^{35,36}. Following that step, using Gaussian 0.9 software equipped with the 6-31G** basis³² values of bond length, dipole moment, heat of formation equal to the energy of dissociation, bond energy HOMO/LUMO energy level for single molecules were again computed using the single-point energy option key word.

Visualisation of the HOMO/LUMO orbitals and changes of the electron density for particular molecules and their three molecule systems was performed involving the HyperChem 8.0 software³⁷ (open-access alternative software: [GaussView 6](#)).

Results and discussion

Molecular oxygen

Properties of the single molecule of oxygen (O₂) situated along the x-axis of the Cartesian system in SMF of the flux density of 0 to 100T are presented in [Table 1](#). Isosurfaces resulting from computations for molecules of the triplet and singlet molecules are presented in [Figure 1](#) and [Figure 2](#), respectively. Energy of electrons situated on particular orbitals in the single molecule of oxygen (O₂) placed in SMF of the flux density of 0 to 100T are collected in [Table 2](#). [Table 3](#) and [Table 4](#) collect data characterizing properties of the system of three molecules of oxygen and HOMO/LUMO energy of the molecules of oxygen building the three molecular system, respectively. Influence of the application of flux density and resulting distribution of corresponding maximum positive and negative charge density in case of three triplet and singlet oxygen molecules are presented in [Figure 3](#) and [Figure 4](#), respectively.

Molecular oxygen in its ground state resided as triplet. Its excitation transformed it into singlet states^{38,39}. They differed from one another in the heat of formation ([Table 1](#)). For the triplet molecule its value was slightly negative whereas for the singlet molecule it was considerably positive. Considerable difference between the values of heat formation of the triplet and singlet molecules reflected the fact that the singlet oxygen was a specific short leaving excited state of oxygen⁴⁰. The bond energy for the triplet as well as singlet molecules slightly decreased with an increase in applied flux density. Corresponding values for the singlet molecules were lower than those for the triplet molecules. The O-O bond length in the triplet molecule was slightly shorter than in the singlet molecule. Therefore, the singlet molecule was more stretched, hence more unstable and reactive. In both cases the bond length fairly regularly increased with an increase in applied flux density. In both cases it resulted in developing residual electric dipole moment more readily in the triplet molecule. Comparison of the energy gaps $\Delta_{\text{HOMO/LUMO}}$ revealed that SMF only slightly influenced the excitation energy of the triplet oxygen molecule but considerably decreased it in the singlet oxygen molecule.

Table 1. Properties of the single molecule of oxygen (O₂) situated along the x-axis of the Cartesian system in SMF of the flux density of 0 to 100T^a.

Property		Flux density [T]				
		0	0.1	1	10	100
Maximal charge density	Positive	0.086 <i>0.255</i>	0.094 <i>0.179</i>	0.105 <i>0.304</i>	0.131 <i>0.198</i>	0.158 <i>0.710</i>
	Negative	-0.080 <i>-0.164</i>	-0.015 <i>-0.085</i>	-0.023 <i>-0.108</i>	-0.101 <i>-0.050</i>	-0.035 <i>-0.104</i>
Bond length [Å]		1.2321 <i>1.2411</i>	1.2324 <i>1.2412</i>	1.2329 <i>1.2415</i>	1.2332 <i>1.2421</i>	1.2336 <i>1.2429</i>
Dipole moment [D]		0 <i>0</i>	0.0001 <i>0.0000</i>	0.0002 <i>0.0000</i>	0.0002 <i>0.0001</i>	0.0003 <i>0.0002</i>
Heat of formation [kcal/mole]		-2.14 <i>106.17</i>	-1.12 <i>108.23</i>	-1.08 <i>109.33</i>	-0.92 <i>115.38</i>	-0.38 <i>127.25</i>
Bond energy [kcal/mole]		498.4 <i>384.5</i>	498.4 <i>384.2</i>	497.6 <i>383.5</i>	489.5 <i>381.1</i>	481.5 <i>372.2</i>
Energy [kcal/mole] LUMO		22.99	18.39	18.12	17.14	15.365
HOMO		21.02	19.95	13.73	12.34	11.88
		11.51 <i>12.83</i>	8.464 <i>12.753</i>	7.23 <i>8.443</i>	4.23 <i>8.419</i>	4.368 <i>9.23</i>
$\Delta_{\text{HOMO/LUMO}}$ [kcal/mol]		11.480 <i>8.190</i>	9.926 <i>7.197</i>	10.890 <i>5.287</i>	12.910 <i>3.921</i>	10.988 <i>2.650</i>

^aUpper and lower (in italics) values are for the triplet and singlet states, respectively.

Figure 1 and Figure 2 present numerically simulated electronic density of so-called isosurfaces, for single molecules of the triplet and singlet oxygen, respectively, exposed to the magnetic field of 0.1 to 100 T along the x-axis. On these and subsequent figures green and pink colours represent positive and negative charge, respectively. The intensity of both colours associated with the value of the charges is scaled on the left side of every isosurface. An increase in applied SMF flux density resulted in polarization of the molecules. The original shape of isosurface of the triplet molecule only slightly changed but in case of the singlet molecule an essential change of the isosurface shape could be noted, particularly at 10 and 100 T.

Values of the maximal negative and positive surface charge densities are grouped in Table 1. In the molecule of triplet oxygen, the maximum of the positive charge density rose regularly against T whereas, simultaneously, the maximum of the negative charge density rose irregularly. The same parameters found for the singlet oxygen molecule also varied irregularly with increase in T. Above 10T a complete shift of the surface charge was observed.

Energy of corresponding LUMO and HOMO of triplet and singlet molecules fairly regularly declined with increase in T (Table 1) but energy of electrons situated on particular orbitals of those molecules varied nonlinearly (Table 2). It might suggest that some flux density dependent hybridizations of corresponding orbitals were involved leading to resonance like structures.

The distribution of the charge presented in structures d and e might suggest formation of ozone.

Like in case of single molecules placed in SMF of 100T also in the group of three singlet as well as triplet molecules the positive and negative charges were distributed symmetrically. Maximal positive charge density for the systems built of three triplet and singlet molecules changed irregularly (Table 3). An initial increase observed for the systems placed in SMF of 0.1 T declined reaching the lowest value for the system placed in SMF of 1 T. This irregularity was well illustrated with specific shapes of corresponding isosurfaces (Figure 3 and Figure 4). In contrast to the maximal positive charge density, maximal negative charge density declined

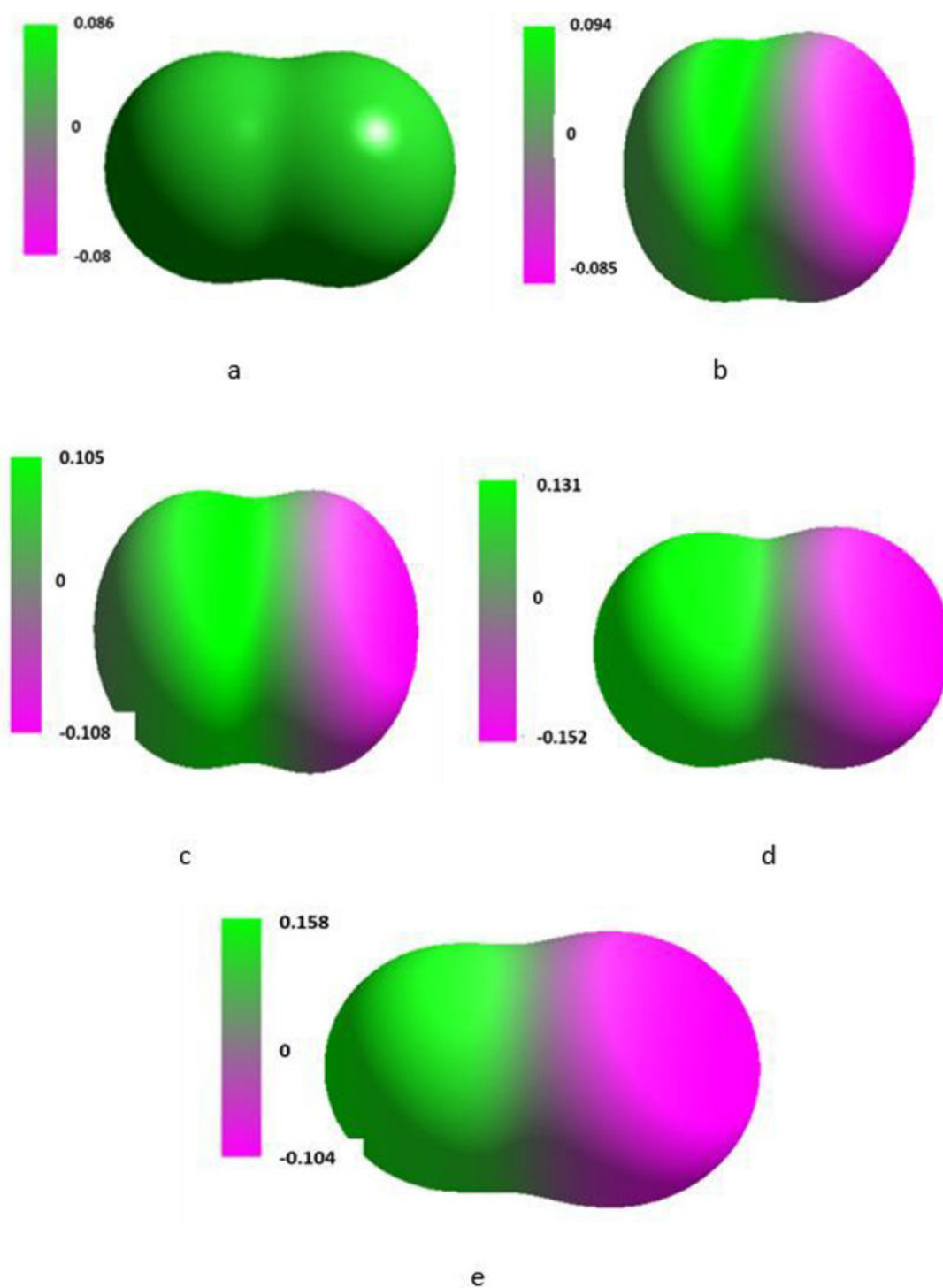


Figure 1. Isosurface along the x-axis of the Cartesian system of the single molecule of triplet oxygen placed in the magnetic field of 0T (**a**), 0.1T (**b**), 1T (**c**), 10T (**d**) and 100T (**e**).

with increase in applied flux density. The irregular pattern of those changes resembled these observed for the maximal

positive charge density. Again, the irregularity was found in the data for the molecules placed in SMF of 1T.

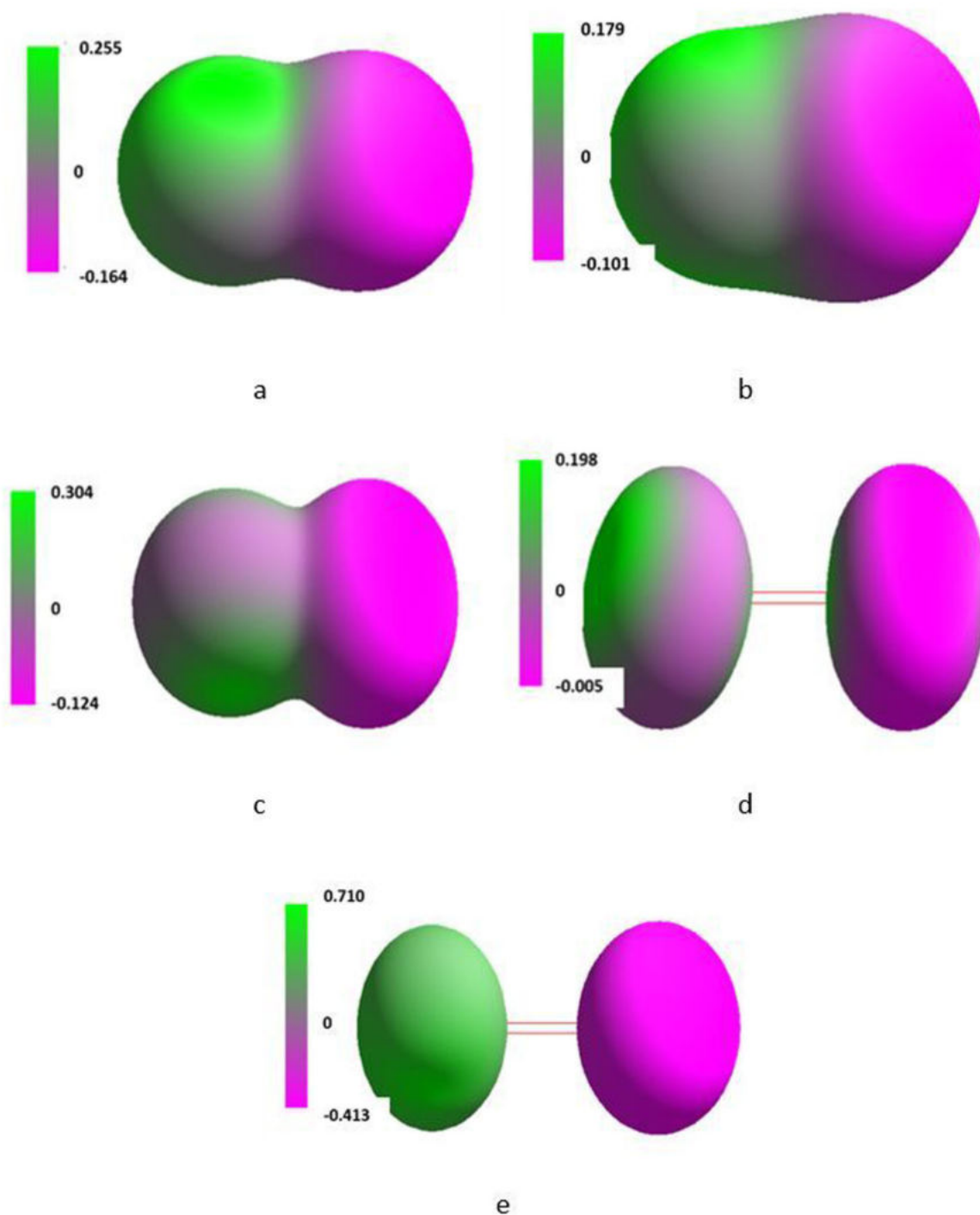


Figure 2. Isosurface along the x-axis of the Cartesian system of the single molecule of singlet oxygen placed in the magnetic field of 0T (**a**), 0.1T (**b**), 1T (**c**), 10T (**d**) and 100T (**e**).

An increase in the SMF flux density shortened and elongated distance between the excited (LUMO) and ground (HOMO) states in the system of three triplet and singlet molecules, respectively (Table 4).

Molecular nitrogen

Corresponding results for single molecules of nitrogen are presented in Table 5 and Table 6 and Figure 5. Data for the system of three molecules of nitrogen are given in Table 7 and

Table 2. Energy of electrons situated on particular orbitals in the single molecule of oxygen (O₂) placed in SMF of the flux density of 0 to 100T^a.

Energy [kcal/mole] at flux density [T]					Orbital
0	0.1	1.0	10	100	
21.02	19.95	13.73	12.34	11.88	↑ π*2p _z ¹
<i>22.99</i>	<i>18.39</i>	<i>18.12</i>	<i>17.14</i>	<i>15.365</i>	
12.83	12.753	8.443	8.419	9.23	↑ π*2p _y ¹
<i>11.51</i>	<i>8.464</i>	<i>7.23</i>	<i>4.23</i>	<i>4.168</i>	
12.84	12.745	8.439	8.412	9.23	↓ π*2p _x ²
<i>11.49</i>	<i>8.463</i>	<i>7.24</i>	<i>4.24</i>	<i>4.156</i>	
-2.796	-2.962	-2.866	-1.985	-1.289	↑↓ π2p _z ²
<i>-10.43</i>	<i>-9.018</i>	<i>-10.62</i>	<i>-10.25</i>	<i>-12.68</i>	
-2.789	-2.968	-2.896	-1.987	-1.286	↑↓ π2p _y ²
<i>-10.56</i>	<i>-9.146</i>	<i>-10.54</i>	<i>-10.52</i>	<i>-12.52</i>	
-7.506	-5.987	-7.435	-7.889	-8.965	↑↓ σ2p _x ²
<i>-31.49</i>	<i>-17.43</i>	<i>-19.27</i>	<i>-16.52</i>	<i>-12.57</i>	
-9.584	-8.346	-8.812	-6.648	-7.218	↑↓ σ*2s ²
<i>-31.11</i>	<i>-17.46</i>	<i>-20.41</i>	<i>-18.25</i>	<i>-26.35</i>	
-11.81	-12.38	-12.45	-10.84	-11.52	↑↓ σ2s ²
<i>-35.38</i>	<i>-19.99</i>	<i>-20.45</i>	<i>-23.57</i>	<i>-27.35</i>	
-18.7	-21.17	-20.97	-20.49	-20.02	↑↓ σ*1s ²
<i>-36.09</i>	<i>-26.36</i>	<i>-25.28</i>	<i>-26.51</i>	<i>-30.17</i>	
-36.28	-35.71	-33.99	-36.14	-36.89	↑↓ σ1s ²
<i>-61.7</i>	<i>-43.24</i>	<i>-42.95</i>	<i>-41.11</i>	<i>-46.98</i>	

^aUpper and lower (in italics) values are for the triplet and singlet states, respectively.

Table 3. Properties of three molecules of oxygen (O₂) situated along the x-axis of the Cartesian system in SMF of the flux density from 0 to 100T^a.

Property		Flux density [T]				
		0	0.1	1	10	100
Maximal charge density	Positive	0.157	0.393	0.220	0.346	0.456
		<i>0.320</i>	<i>0.592</i>	<i>1.267</i>	<i>0.362</i>	<i>0.456</i>
	Negative	-0.137	-0.141	-0.136	-0.271	-0.385
		<i>-0.176</i>	<i>-0.274</i>	<i>-0.377</i>	<i>-0.247</i>	<i>-0.360</i>
Total energy [kcal/mole]		321.56	322.54	346.75	351.87	367.25
		<i>12.25</i>	<i>16.89</i>	<i>19.58</i>	<i>26.58</i>	<i>36.89</i>

^aValues in normal font and italics are for the triplet and singlet states, respectively.

Table 8 and in Figure 6. Molecular nitrogen in the ground state is in the singlet state but under specific conditions it can be excited into triplet states^{41,42}. SMF of the flux density increasing up to 100T only slightly changed properties of that

molecule retaining its singlet character (Table 5). The interatomic distance slightly increased and the residual dipole moment generated already at 1T remained practically unchanged up to 100T. As the applied T increased, heat of formation of

Table 4. HOMO/LUMO energy in the three molecules of oxygen (O_2) placed in SMF of the flux density of 0 to 100T^a.

Parameter	Energy [kcal/mole] at flux density [T]				
	0	0.1	1	10	100
LUMO	33.12	28.32	27.58	27.11	25.14
	<i>43.99</i>	<i>41.59</i>	<i>41.25</i>	<i>44.68</i>	<i>46.85</i>
HOMO	21.23	20.75	20.23	21.56	19.57
	<i>24.59</i>	<i>21.02</i>	<i>20.36</i>	<i>20.56</i>	<i>21.32</i>
$\Delta_{\text{HOMO/LUMO}}$	11.89	7.57	7.35	5.55	5.57
	<i>19.4</i>	<i>20.57</i>	<i>20.89</i>	<i>24.12</i>	<i>25.53</i>

^aUpper and lower (in italics) values are for the triplet and singlet states, respectively.

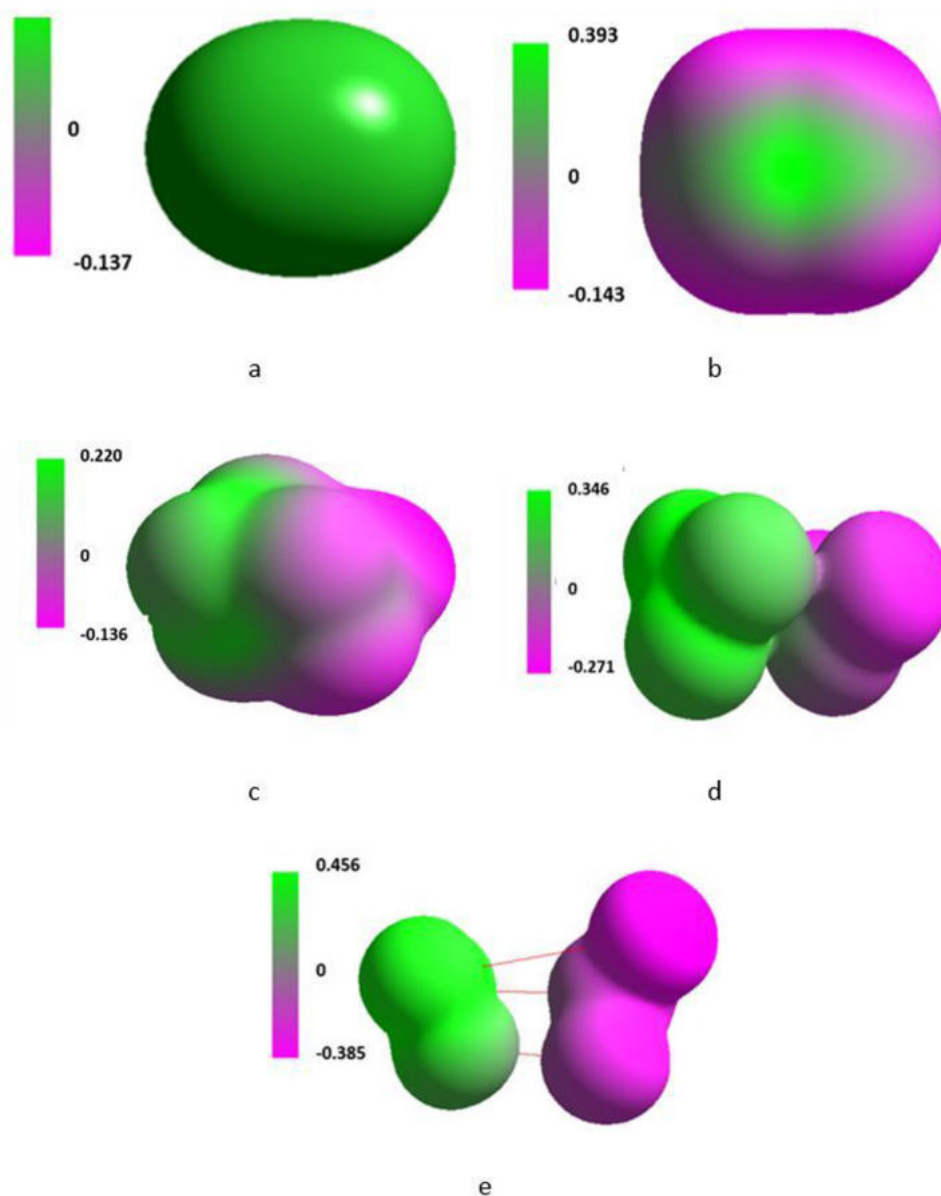


Figure 3. Isosurface along the x-axis of the Cartesian system of three molecules of triplet oxygen placed in the flux density of 0T (a), 0.1T (b), 1T (c), 10T (d) and 100T (e).

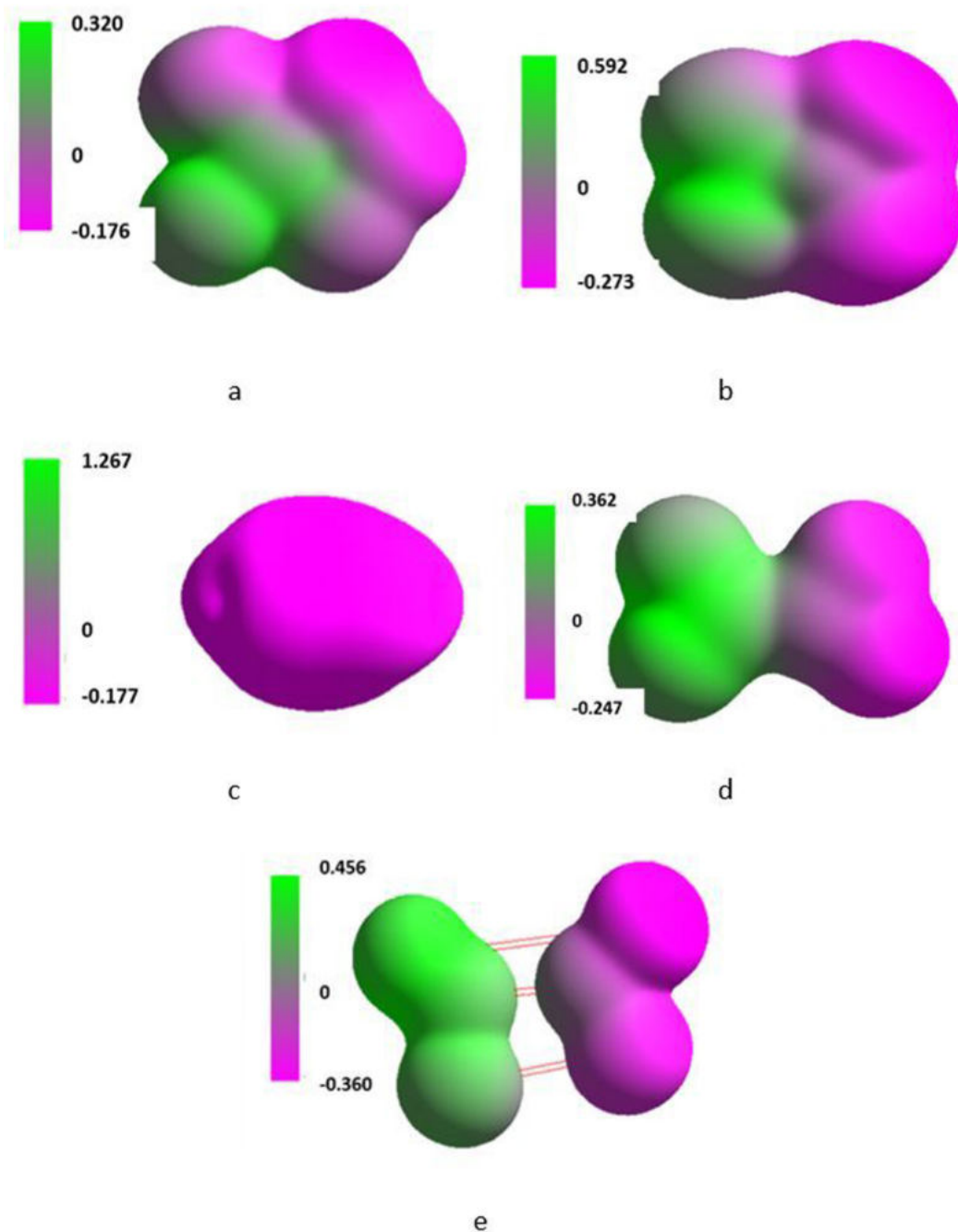


Figure 4. Isosurface along the x-axis of the Cartesian system of three molecules of singlet oxygen placed in the flux density of 0T (a), 0.1T (b), 1T (c), 10T (d) and 100T (e).

the molecule considerably increased and, simultaneously, bond energy decreased. The energy of LUMO initially slightly decreased in order to increase the flux density of 10 and 100T. It was paralleled with a regular decrease in the energy of HOMO. An insight into energy of electrons situated on particular orbitals in the single molecule of nitrogen (N_2) (Table 6)

revealed that, with some exceptions, they changed regularly against increasing values of T. The irregularities were noted in case of the π^*2p , σ^*2s and σ^*1s orbitals at 0.1 and 1T. They might be associated with the SMF promoted hybridization of those orbitals. An increase in $\Delta_{\text{HOMO/LUMO}}$ informs that an increase in SMF flux density resulted in inhibiting excitation of the

Table 5. Properties of the single molecule of nitrogen (N_2) situated along the x-axis of the Cartesian system in SMF of the flux density from 0 to 100T.

Property		Flux density [T]				
		0	0.1	1	10	100
Maximal charge density	Positive	0.246	0.326	0.316	0.331	0.333
	Negative	-0.094	-0.068	-0.151	-0.160	-0.250
Bond length [\AA]		1.0912	1.0913	1.0923	1.0932	1.0936
Dipole moment [D]		0	0	0.0001	0.0001	0.0001
Heat of formation [kcal/mole]		-1.05	-1.04	-0.95	-0.23	-0.19
Bond energy [kcal/mole]		906.2	906.2	901.3	898.7	896.3
Energy [kcal/mole] LUMO		6.57	6.382	6.349	7.324	8.256
HOMO		-1.043	-1.364	-1.811	-1.912	-1.950
Δ HOMO/LUMO [kcal/mole]		7.613	7.746	8.16	9.236	10.206

Table 6. Energy of electrons situated on particular orbitals in the single molecule of nitrogen (N_2) placed in SMF of the flux density of 0 to 100T.

Energy [kcal/mole] at flux density [T]					Orbital
0	0.1	1.0	10	100	
6.58	6.382	6.334	7.321	8.256	$\uparrow\downarrow \pi^*2p_z^2$
6.57	6.382	6.349	7.324	8.256	$\uparrow\downarrow \pi^*2p_y^2$
-1.043	-1.364	-1.811	-1.912	-1.950	$\uparrow\downarrow \pi 2p_z^2$
-3.685	-4.235	-5.48	-5.98	-6.02	$\uparrow\downarrow \pi 2p_y^2$
-3.681	-4.236	-5.46	-5.98	-6.02	$\uparrow\downarrow \sigma 2p_x^2$
-14.31	-13.25	-12.43	-12.89	-12.96	$\uparrow\downarrow \sigma^* 2s^2$
-16.25	-17.25	-18.82	-20.68	-21.28	$\uparrow\downarrow \sigma 2s^2$
-21.41	-21.25	-22.45	-22.84	-22.92	$\uparrow\downarrow \sigma^* 1s^2$
-41.52	-41.53	-41.97	-41.97	-42.02	$\uparrow\downarrow \sigma 1s^2$

molecule. It also increased and decreased maximum of the positive and negative charge density, respectively (Table 4), however, as shown in Figure 5 the size and shape of the isosurface along the x-axis remained fairly stable.

In the system of three nitrogen molecules its total energy rose with applied flux density. Energy of LUMO and HOMO of the whole system increased and decreased, respectively (Table 7). Difference between energy of HOMO and LUMO was independent of applied SMF. Maximum of the positive and

negative charge density distribution quoted in Table 7 reflected substantial changes of the shape and size of the isosurface presented in Figure 6.

On increase in applied T maximum of the positive charge on the surface increased by 0.220 units. Simultaneously, maximum of the negative charge density decreased by 0.221 units. Thus, the charge shifts proceeded solely on the surface. Because the sum of both values was close to zero the charge did not delocalize.

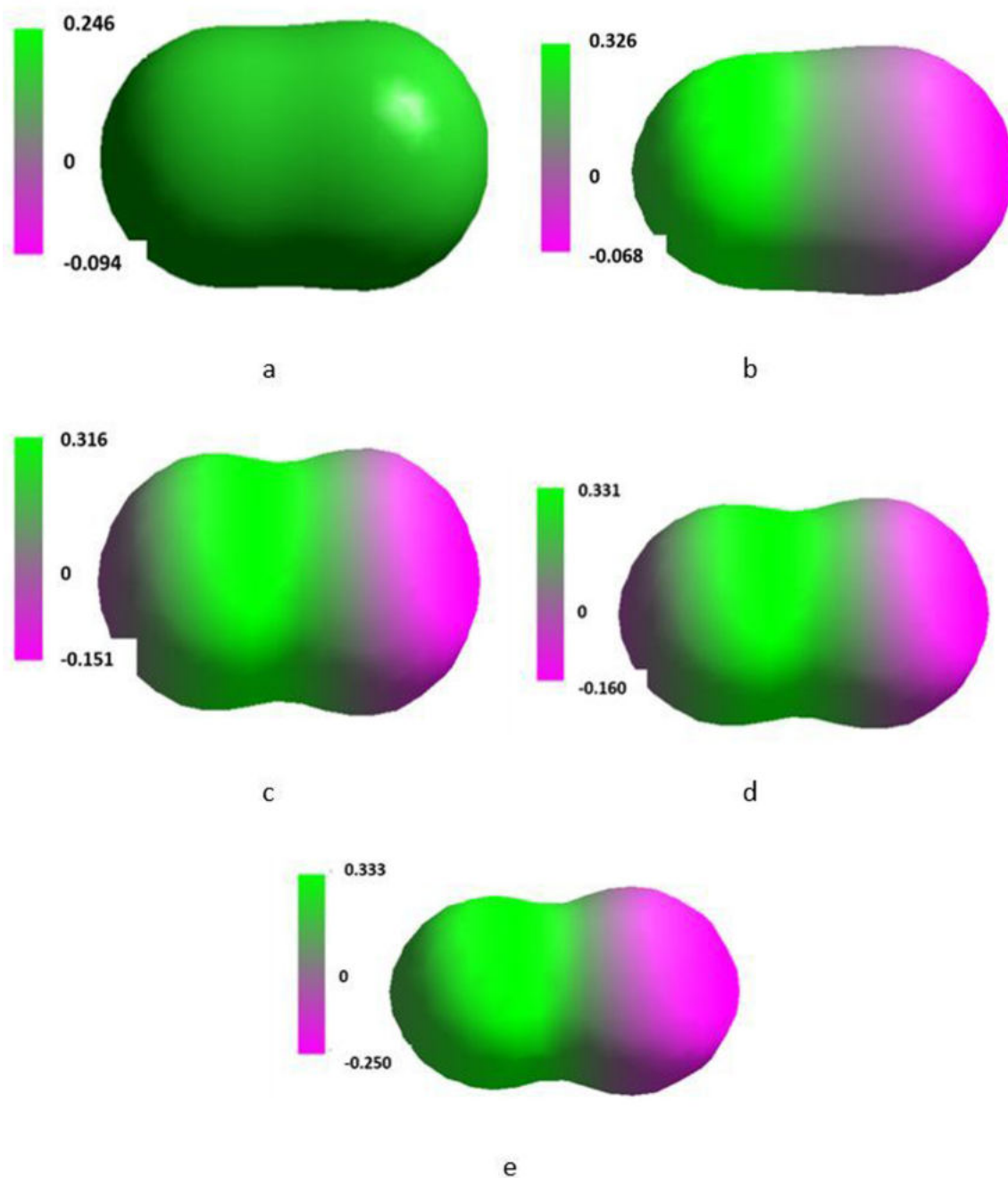


Figure 5. Isosurface along the x-axis of the Cartesian system of the single molecule of nitrogen placed in the SMF flux density of 0T (a), 0.1T (b), 1T (c), 10T (d) and 100T (e).

Table 7. Total, LUMO and HOMO energy of the system composed of three molecules of nitrogen placed in SMF of the flux density of 0 to 100T.

Parameter	Energy [kcal/mole] at flux density [T]				
	0	0.1	1	10	100
Total	307.23	315.68	324.58	368.59	446.26
LUMO	29.52	29.59	30.25	31.38	33.85
HOMO	-11.52	-11.02	-10.36	-10.22	-10.12
$\Delta_{\text{HOMO/LUMO}}$	41.04	40.61	40.61	41.60	43.97

Table 8. Maximum of the positive and negative charge density distribution in the system of three molecules of nitrogen (N_2) placed in SMF of the flux density of 0 to 100T.

Charge	Maximal charge density at flux density [T]				
	0	0.1	1.0	10	100
Positive	+0.479	+4.498	+0.502	+0.527	+0.699
Negative	-0.132	-0.295	-0.211	-0.118	-0.353

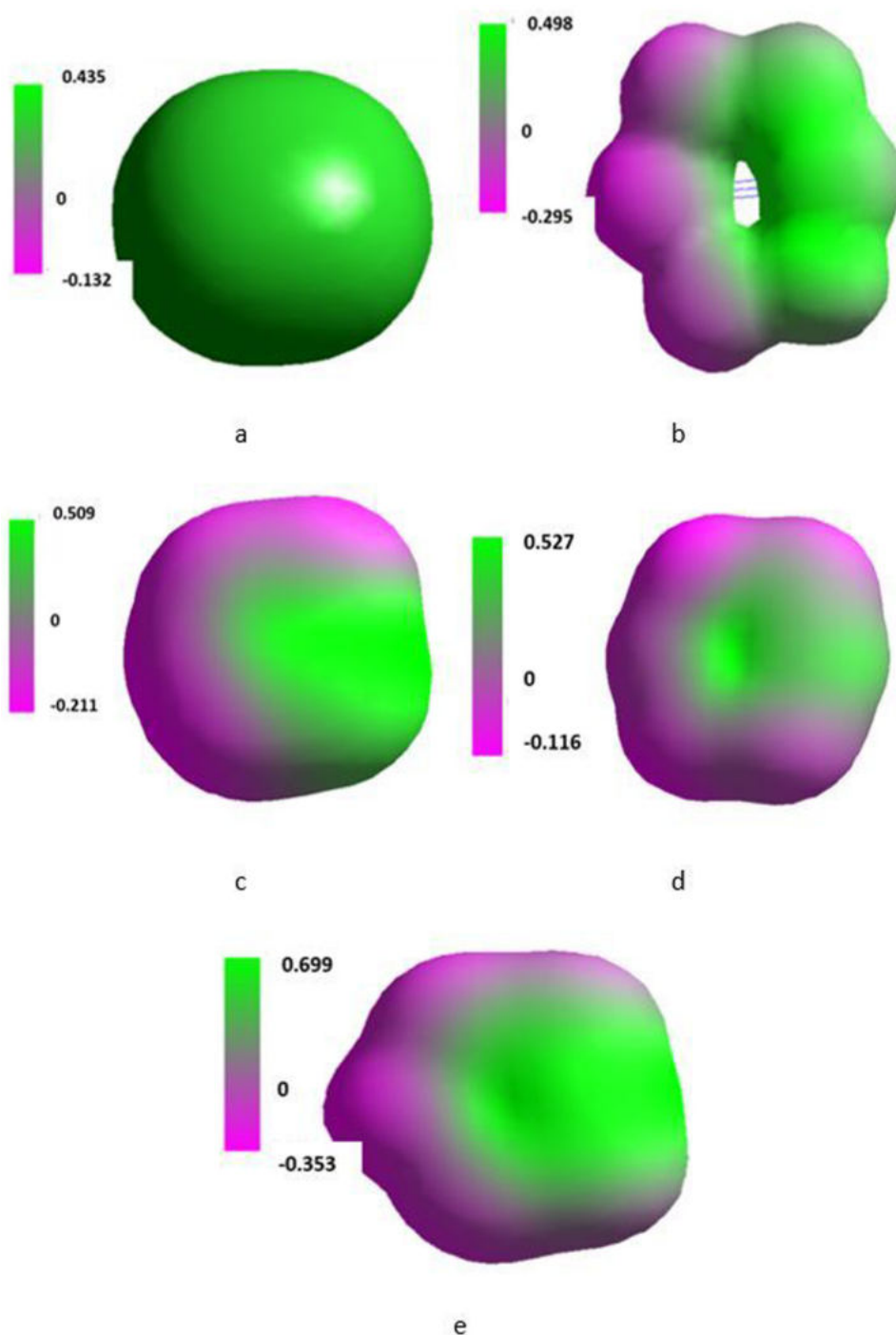


Figure 6. Isosurface along the x-axis of the Cartesian system of three molecules of nitrogen placed in the SMF flux density of 0T (a), 0.1T (b), 1T (c), 10T (d) and 100T (e).

Depending on the applied flux density, the system of three nitrogen molecules reoriented in the Cartesian system as shown in Figure 6. It was accompanied with a fluctuation of the value of the maximum negative charge density (Table 8).

Water

Table 9 and Table 10 and Figure 7 contain results of computations for a single molecule of water and Figure 8 shows its isosurface. Subsequently, data for the system of three molecules of water are given in Table 11 and Table 12, and the isosurface for that system is presented in Figure 9. In nature, above 0K, water molecules vibrate like other molecules. The O-H bond lengths change either symmetrically

or asymmetrically. It is reflected by changes of their dipole moment. In consequence, their hydrophilic/hydrophobic properties are accordingly modified. Such vibrations also affect dissociation of the molecules influencing their ability to build the macrostructure with involvement of intermolecular hydrogen bonds. Additionally, bending modes change the H-O-H bond angle of these molecules⁴³.

Computations for the water molecule placed under computer vacuum in SMF could potentially suggest a facile H-O-H bond break and the ability to form intermolecular hydrogen bonds. If lone electron pairs at the oxygen atom were activated an increase in basicity of the water molecule could be considered.

Table 9. Properties of the single molecule of water situated along the x-axis of the Cartesian system in SMF of the flux density from 0 to 100T.

Property		Flux density [T]				
		0	0.1	1	10	100
Maximal charge density	Positive	0.934	0.933	1.213	1.202	1.231
	Negative	0.151	0.150	0.215	0.699	0.702
Bond length [Å]	O-H1	0.9591	0.9605	0.9657	0.9659	0.9691
	O-H2	0.9591	0.9605	0.9605	0.9591	0.9591
	O-H1	0.9591	0.9605	0.9657	0.9659	0.9691
	O-H2	0.9591	0.9605	0.9605	0.9591	0.9591
Dipole moment [D]		1.845	1.846	1.849	1.851	1.862
Heat of formation [kcal/mole]		-285.2	-284.7	-283.5	-282.8	-280.1
Bond energy [kcal/mole]		461.5	461.3	457.5	456.3	454.3
Energy [kcal/mole] LUMO		11.01	11.23	11.62	11.71	11.85
HOMO		-4.137	-4.124	-4.151	-4.169	-4.178
$\Delta_{\text{HOMO/LUMO}}$ [kcal/mol]		15.147	15.354	15.771	15.879	16.028

Table 10. Energy of electrons situated on selected orbitals in the single molecule of water placed in SMF of the flux density of 0 to 100T.

Energy [kcal/mole] at flux density [T]					
0	0.1	1.0	10	100	Orbital ^a
11.01	11.23	11.62	11.71	11.85	3a1
-4.137	-4.138	-4.151	-4.169	-4.178	↑↓ 1b1
-6.165	-6.169	-6.172	-6.173	-6.175	↑↓ 2a1
-10.93	-11.36	-11.39	-11.42	-11.49	↑↓ 1b2
-25.23	-25.26	-25.31	-25.36	-25.41	↑↓ 1a1

^aSee Figure 7 for notation.

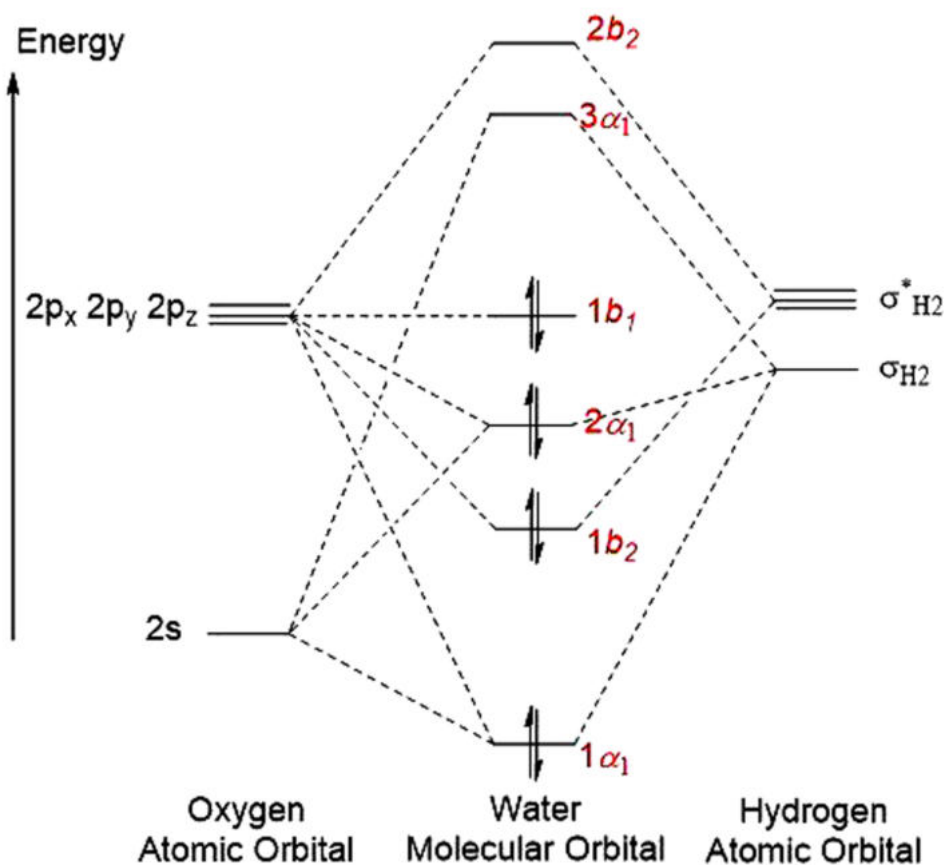


Figure 7. Notation of assignments of orbitals in Table 10.

As shown in Table 9, SMF of the flux density of 0.1T symmetrically elongated both O-H bonds and that symmetry ceased at 1 to 100T. That treatment provided moderate increase in dipole moment of the molecule, monotonous decrease in the bond energy and stability of the molecule in terms of increasing its heat of formation. However, it should be noted that starting from 10T the length of the first of the O-H bonds decreased. It pointed to an involvement of decrease in the symmetry of vibrations, whereas vibrations of the second O-H bond remained nearly constant.

An increase in the flux density was paralleled with increase in the positive energy of LUMO and negative energy of HOMO. Monotonous increase in $\Delta_{\text{HOMO/LUMO}}$ values showed that an increase in the SMF flux density reduced a possibility of excitation of the water molecule. Energy of electrons on particular orbitals in the single water molecule varied with the flux density in the manner presented in Table 10. Solely the positive energy of the empty $3a_1$ orbital monotonously increased against increasing flux density whereas the negative energy of electrons occupying remaining orbitals slightly

monotonously declined. It pointed to inhibiting excitation of the water molecule.

Isosurface along the x-axis of the Cartesian system for the single molecule of water (Figure 8) demonstrated that SMF only slightly changed orientation of the molecule with increase in the surface density but polarization of the molecule considerably increased.

Total energy of the system built of three molecules of water was fairly insensitive to an increase in applied flux density. Moreover, there was considerable response from the energy of LUMO and HOMO. The energy of LUMO monotonously increased and, simultaneously, energy of HOMO in the same manner decreased (Table 11) as demonstrated in terms of an increase in $\Delta_{\text{HOMO/LUMO}}$. Thus, SMF inhibited the excitation of the molecule of water.

Maximum of the positive and negative charge density distribution quoted in Table 12 reflected substantial changes of the shape and size of the isosurface presented in Figure 9.

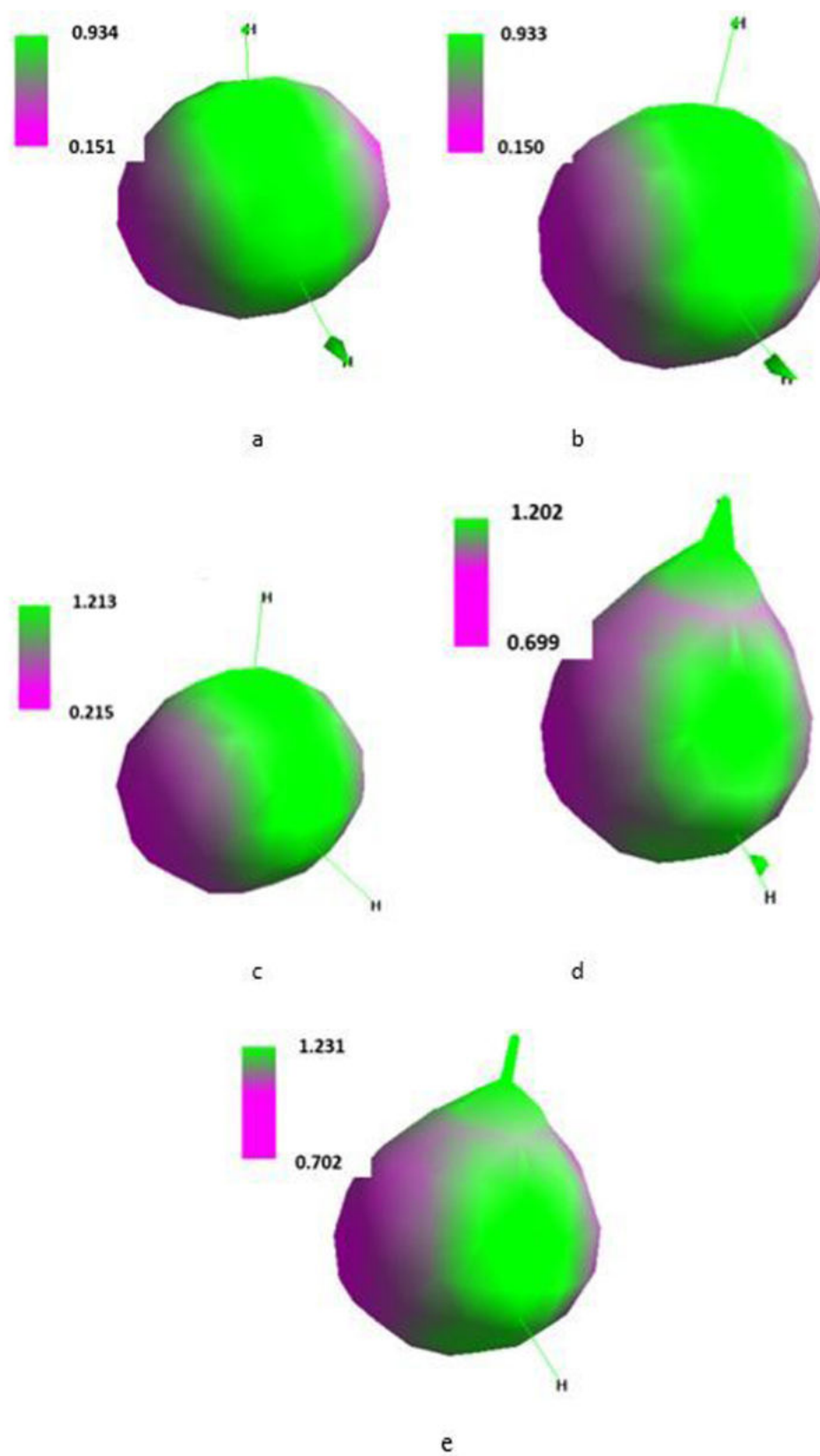


Figure 8. Isosurface along the x-axis of the Cartesian system of the single molecule of water placed in the SMF flux density of 0T (a), 0.1T (b), 1T (c), 10T (d) and 100T (e).

Table 11. Total, LUMO and HOMO energy of the system composed of three molecules of water placed in SMF of the flux density of 0 to 100T.

Parameter	Energy [kcal/mole] at flux density [T]				
	0	0.1	1	10	100
Total	156.3	156.8	157.3	159.6	161.8
LUMO	5.17	5.51	6.21	6.88	7.85
HOMO	-2.14	-2.07	-1.53	-1.22	-1.12
$\Delta_{\text{HOMO/LUMO}}$	7.31	7.58	7.74	8.10	8.97

Table 12. Maximum of the positive and negative charge density distribution in the system of three water molecules placed in SMF of the flux density of 0 to 100T.

Charge	Maximal charge density at flux density [T]				
	0	0.1	1.0	10	100
Positive	1.621	2.248	3.522	30.656	2.301
Negative	0.545	0.470	0.446	0.318	0.456

Out of SMF, three water molecules arranged into an irregular ball. At 0.1T it polarized with simultaneous reorientation along the x-axis. Its shape was retained but as the flux density increased, it gradually expanded into a more linear shape in which the number of intermolecular hydrogen bonds declined. A considerable irregularity in the distribution of the maximum charge density at 10T should be noted. It was reflected by a specific shape of the corresponding isosurface (Figure 9).

Carbon dioxide

Table 13, Table 14 and Figure 10 and Figure 11 present relevant data for a single CO₂ molecule. and Table 15, Table 16 and Figure 12 show computed data for the system of three CO₂ molecules.

Carbon dioxide represents a π -electron system. Hence, because of the mobility of the π -electrons^{44,45} unexpected behaviour of the molecule placed in SMF might be anticipated. Thus, the length of both C=O bonds changed with increase in T but at 0.1 and 100T both bonds had slightly different length, perhaps mainly because of limited precision of calculations. Dipole moment of the molecule increased with T whereas the heat of formation and bond energy practically linearly decreased against T (Table 13). Energy of LUMO and HOMO also monotonously increased and decreased, respectively. The energetic $\Delta_{\text{HOMO/LUMO}}$ gap reached maximum at about 1T.

Irregularity was observed for changes of maximum of positive and negative charge density (Table 13). Maximum of positive charge density increased up to 1T in order to strongly decrease at 10 and 100T. Except electrons situated at 2b_{2u}, level energy of electrons situated on particular orbitals of the single molecule at increasing SMF flux density only slightly changed. Energy of electrons located at the 2b_{2u} jumped suddenly at 1T (Table 14).

Shape of isosurface of the SMF treated molecule (Figure 11) resulted in polarisation of the molecule in varying manner tending to localize the negative charge on the oxygen atoms. The effect was dependent on the applied flux density. The molecules did not reorient in the Cartesian system holding their initial orientation.

In the system composed of three CO₂ molecules, total energy of the system increased with an increase in applied flux density. The LUMO energy reached maximum at 0.1T in order to decrease up to 100T. Energy of HOMO changed in the same way (Table 15).

Maximum of the positive and negative charge density distribution (Table 16) reflected substantial changes of the shape and size of the isosurface presented in Figure 12. Three molecules of CO₂ out of SMF formed a ball. In the SMF of 0.1T a tendency to separate that ball into two parts perpendicularly to the x-axis was observed. This tendency increased with increase in applied T in order to afford a separation at 100T.

Ammonia

Results for a single molecule of ammonia are given in Table 17 and Table 18 and in Figure 13 and Figure 14. Data for the system of three molecules of ammonia can be found in Table 19 and Table 20 and in Figure 15.

The molecule is the shape of a pyramid with the orbital occupied by the lone electron pair and it is also capable of excitation⁴⁶. When placed in SMF the bond lengths responded depending on the applied flux density. At 1 to 100T their lengths gradually compressed to an extent individual to each bond (Table 17). Nevertheless, the N-H bonds turned shorter, dipole moment slightly increased paralleling applied flux density. These changes were paralleled by increase in heat of formation and decrease in bond energy.

An increase in the SMF flux density resulted in an increase in the $\Delta_{\text{HOMO/LUMO}}$ energy. Thus, SMF deactivates ammonia. Simultaneously, energy of LUMO and HOMO proportionally increased and decreased, respectively.

Maximum of the positive charge density rapidly jumped after application of 0.1T and then rose regularly with increase in applied T (Table 17). This jump was accompanied by a similar jump of the maximum of the negative charge density.

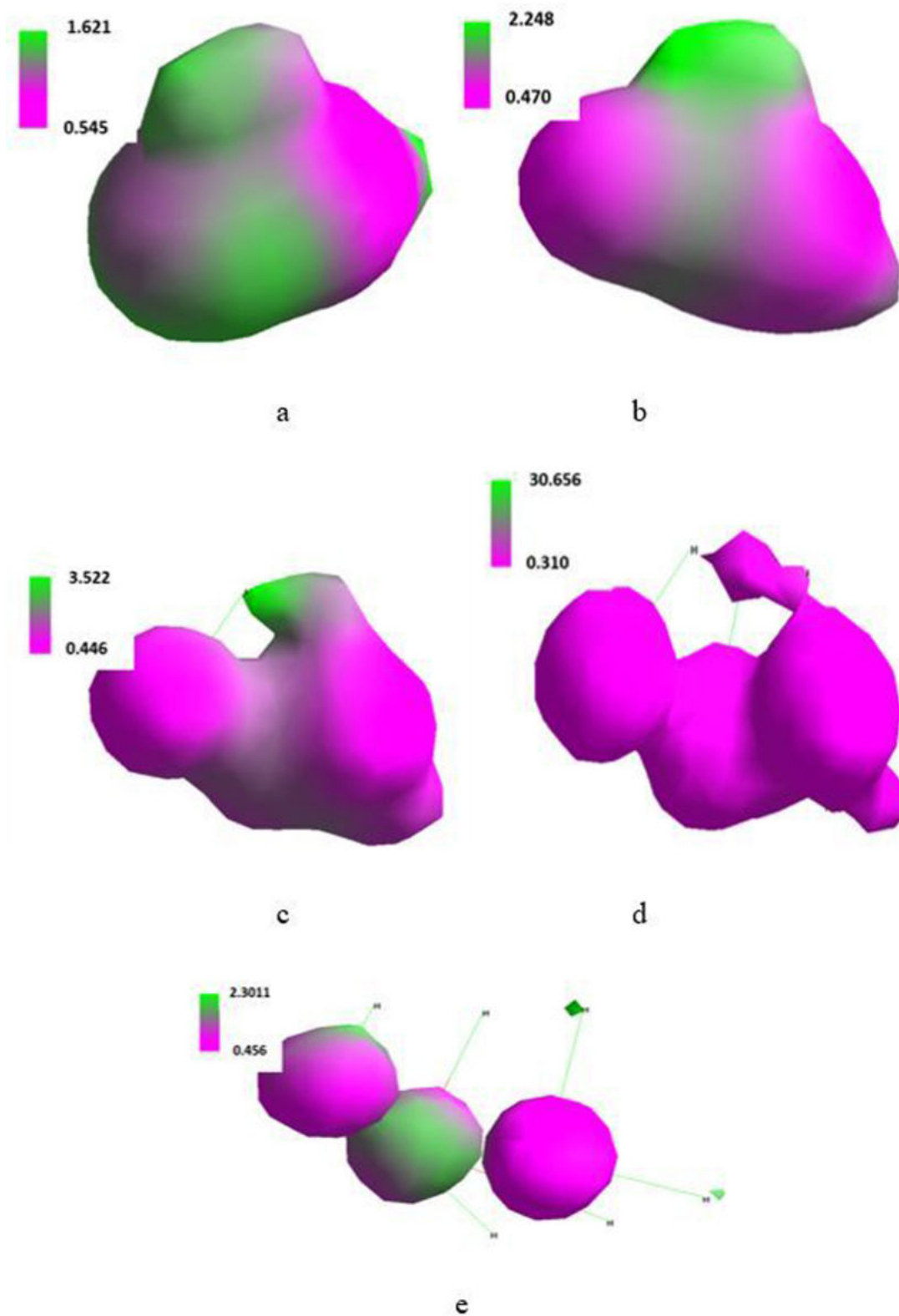


Figure 9. Isosurface along the x-axis of the Cartesian system of three molecules of water placed in the SMF flux density of 0T (a), 0.1T (b), 1T (c), 10T (d) and 100T (e).

Table 13. Properties of the single molecule of CO₂ situated along the x-axis of the Cartesian system in SMF field of the flux density from 0 to 100T.

Property		Flux density [T]				
		0	0.1	1	10	100
Maximal charge density	Positive	3.615	3.968	5.281	1.839	1.718
	Negative	0.493	0.632	0.042	-0.204	-0.221
Bond length [Å]	C-O1	1.16012	1.16015	1.16026	1.1603	1.1604
	C-O2	1.16012	1.16014	1.16026	1.1603	1.1604
Dipole moment [D]		0	0.0010	0.0012	0.0016	0.0033
Heat of formation [kcal/mole]		-285.49	-285.11	-284.25	-281.11	-276.23
Bond energy [kcal/mole]		816.2	816.1	814.5	811.4	803.5
Energy [kcal/mole]	LUMO	1.235	1.435	1.635	1.735	1.896
	HOMO	-4.424	-4.413	-4.369	-3.559	-3.424
$\Delta_{\text{HOMO/LUMO}}$ [kcal/mole]		5.659	5,848	6.019	5,294	5,320

Table 14. Energy of electrons situated on particular orbitals in the single molecule of CO₂ placed in SMF of the flux density of 0 to 100T.

Energy [kcal/mole] at flux density [T]					Orbital ^a
0	0.1	1.0	10	100	
1.235	1.435	1.635	1.735	1.896	↑↓ 3b _{1u}
-4.424	-4.413	-4.369	-3.569	-3.424	↑↓ 1b _{3g}
-4.424	-4.413	-4.366	-3.566	-3.422	↑↓ 1b _{3g}
-7.245	-7.643	-9.474	-9.854	-9.995	↑↓ 2b _{2u}
-7.247	-7.635	-9.459	-9.855	-9.997	↑↓ 2b _{2u}
-9.470	-9.684	-10.240	-11.230	-12.470	↑↓ 2b _{1u}
-12.42	-12.46	-12.87	-13.04	-13.42	↑↓ 2a _g
-27.45	-27.47	-27.56	-27.62	-29.45	↑↓ 1b _{1u}
-29.36	-29.43	-30.09	-30.13	-32.36	↑↓ 1a _g

^aSee Figure 10 for notation.

However, as the applied flux density increased, the value of the maximum charge density decreased. From the data for energy of electrons placed in SMF (Table 18), electrons situated on orbitals 1e could be involved. The molecule situated in the Cartesian system along the x-axis only slightly rotated under the influence of increasing flux density (Figure 14).

In the system of three ammonia molecules its total energy increased with increase in the SMF flux density whereas energy of LUMO monotonously decreased. Simultaneously, energy

of HOMO monotonously increased up to 10T in order to slightly decrease at 100T (Table 19). A monotonously decreasing $\Delta_{\text{HOMO/LUMO}}$ showed that an increase in the SMF flux density favoured excitation of the system. Maximum of the positive and negative charge density distribution quoted in Table 20 reflected substantial changes of the shape and size of the isosurface presented in Figure 15.

The change of the shape of isosurface of the system of three molecules of NH₃ (Figure 15) suggested that in the system

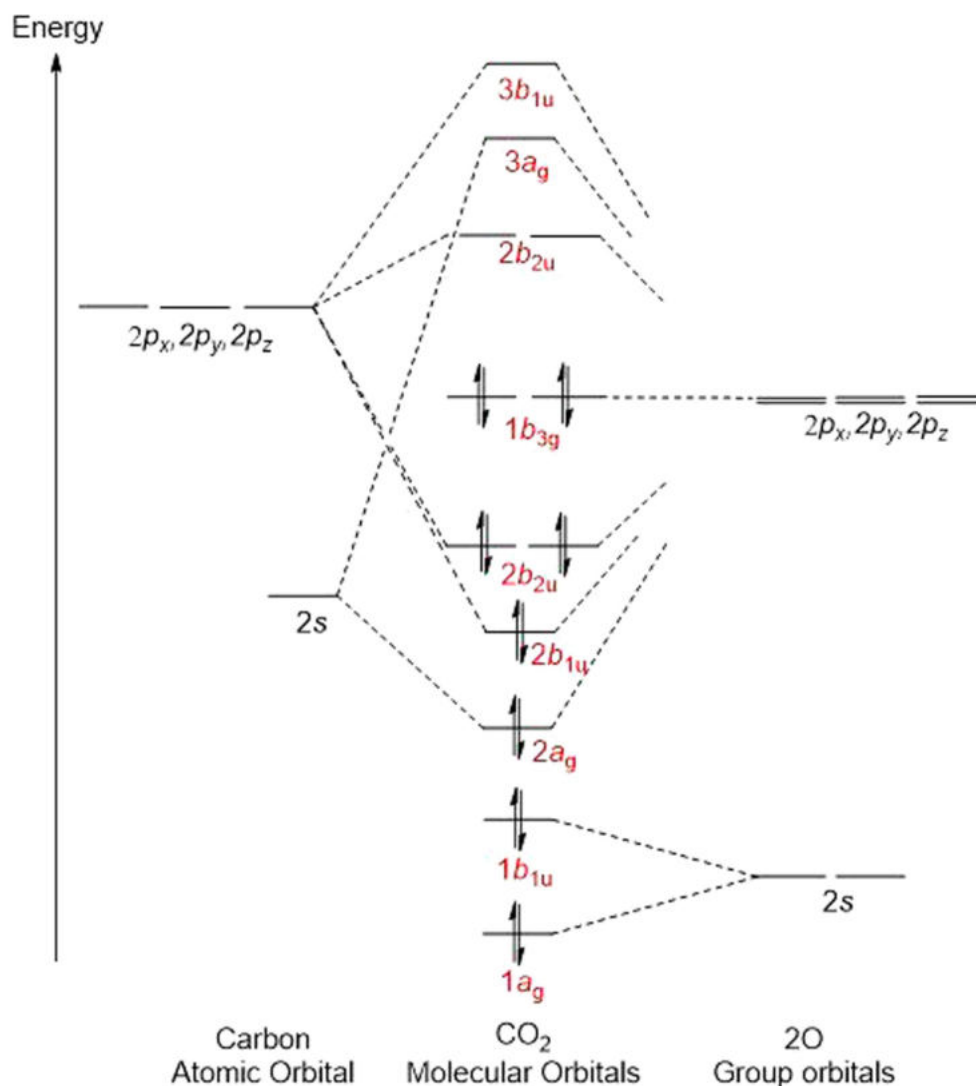


Figure 10. Notation of assignments of orbitals in Table 14.

out of SMF the molecules interacted involving polar and van der Waals forces. Increasing flux density deteriorated these interactions leading to separated mutually non-interacting molecules.

Methane

Computed data for a single molecule of methane are placed in Table 21 and Table 12 and in Figure 16 and Figure 17, whereas corresponding data for the system of three molecules of methane are given in Table 23 and Table 24 and in Figure 18.

Methane presents a symmetric tetrahedron with the carbon atom in its geometrical center and four hydrogen atoms in its

corners. Some low-laying electronic excited states of the molecule were computed with the *ab initio* method⁴⁷.

Low polarization of the C-H bonds makes the whole molecule fairly resistant to SMF. Just the flux density of 10T slightly expanded the C-H bonds from 1.0932 to 1.0936 (two of four C-H bonds) and to 1.0938Å (remaining two bonds). Increase in the flux density to 100T produced further, non-symmetric elongation of the C-H bonds (Table 21). It resulted in generation of a residual dipole moment of the molecule. However, an increase in the heat of formation could be noted already on exposure of the molecule to 1T. It was accompanied with a slight decrease in the bond energy. Changes of maximum positive and negative charge density appeared

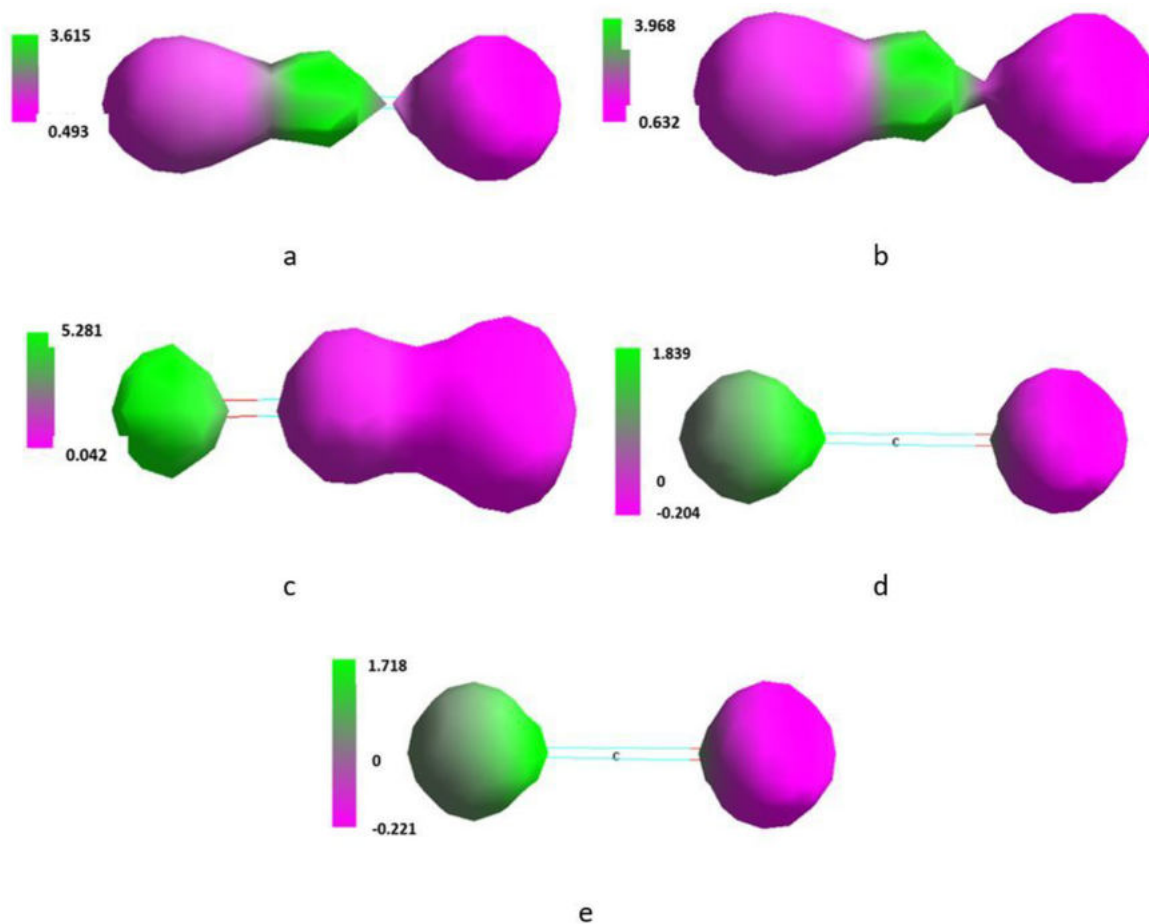


Figure 11. Isosurface along the x-axis of the Cartesian system of the single molecule of CO_2 placed in SMF flux density of 0T (a), 0.1T (b), 1T (c), 10T (d) and 100T (e).

Table 15. Total, LUMO and HOMO energy of the system composed of three molecules of CO_2 placed in SMF of the flux density of 0 to 100T.

Parameter	Energy [kcal/mole] at flux density [T]				
	0	0.1	1	10	100
Total	317.23	319.38	324.58	358.44	387.98
LUMO	4.47	4.51	4.21	3.88	3.85
HOMO	-3.64	-3.67	-3.53	-3.22	-3.12
$\Delta_{\text{HOMO/LUMO}}$	8.11	7.81	7.74	7.10	6.97

Table 16. Maximum of the positive and negative charge density distribution in the system of three CO_2 molecules placed in SMF flux density of 0 to 100T.

Charge	Maximal charge density at flux density [T]				
	0	0.1	1.0	10	100
Positive	1.282	1.981	1.710	9.643	6.801
Negative	0.214	0.370	-0.003	0.888	-0.123

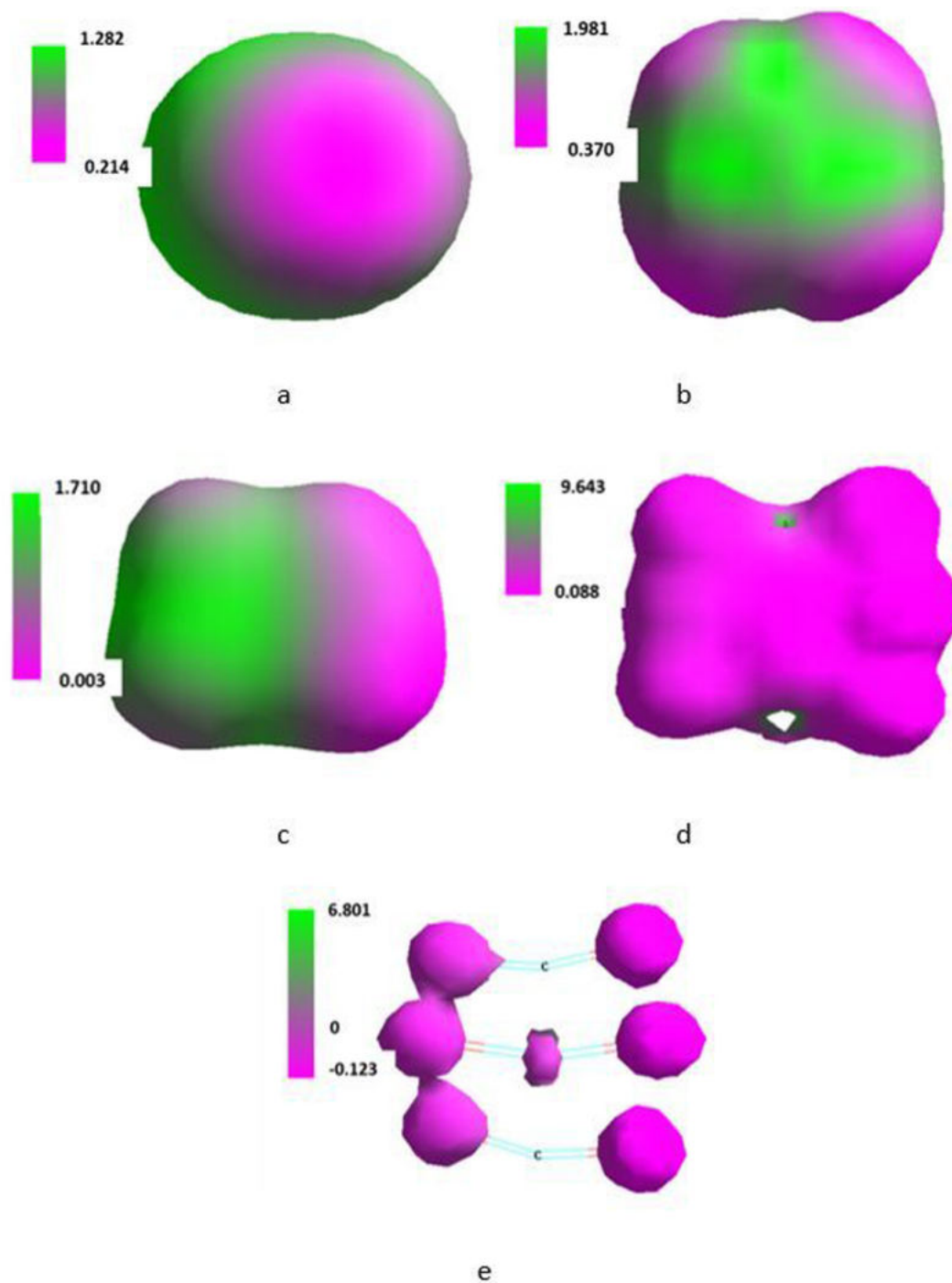


Figure 12. Isosurface along the x-axis of the Cartesian system of three molecules of CO₂ placed in SMF flux density of 0T (**a**), 0.1T (**b**), 1T (**c**), 10T (**d**) and 100T (**e**).

peculiar. They were accompanied neither by specific changes of the LUMO and HOMO energy (Table 21) nor energy of electrons situated on particular orbitals of that

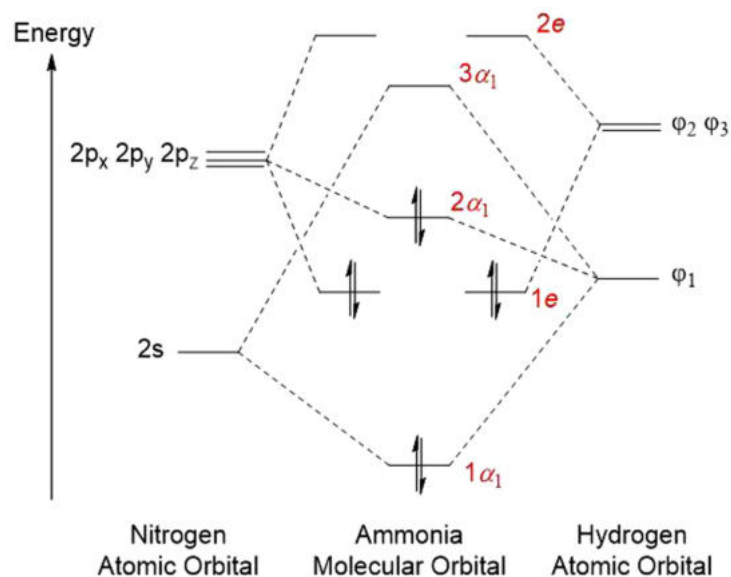
molecule (Table 22). A monotonous increase in $\Delta_{\text{HOMO/LUMO}}$ with increasing SMF flux density pointed to reduced affinity of methane to activation. The $3a_1$ level corresponded to

Table 17. Properties of the single molecule of NH₃ situated along the x-axis of the Cartesian system in SFM of the flux density of 0 to 100T.

Property		Flux density [T]				
		0	0.1	1	10	100
Maximal charge density	Positive	2.643	5.232	5.856	6.028	6.534
	Negative	0.979	1.165	1.118	0.677	0.465
Bond length [Å] N-H1		1.00825	1.00802	1.007885	1.007852	1.00782
	N-H2	1.00825	1.00803	1.007881	1.007620	1.00783
	N-H3	1.00825	1.00803	1.007886	1.007596	1.00782
Dipole moment [D]		1.43	1.43	1.47	1.49	1.56
Heat of formation [kcal/mole]		-46.98	-45.02	-42.01	-36.85	-31.42
Bond energy [kcal/mole]		391.2	390.3	387.2	384.7	381.3
Energy [kcal/mole] LUMO		5.229	5.232	5.856	6.028	6.534
	HOMO	-5.029	-5.098	-5.625	-5.874	-6.125
$\Delta_{\text{HOMO/LUMO}}$ [kcal/mole]		10.258	10.330	11.481	11.902	12.659

Table 18. Energy of electrons situated on particular orbitals in the single molecule of NH₃ placed in SMF of the flux density of 0 to 100T.

Energy [kcal/mole] at flux density [T]					
0	0.1	1.0	10	100	Orbital ^a
5.229	5.232	5.856	6.028	6.534	3a ₁
-5.092	-5.098	-5.625	-5.874	-6.125	↑↓ 2a ₁
-11.64	-11.56	-11.45	-11.14	-10.25	↑↓ 1e
-11.62	-11.54	-11.45	-11.15	-10.23	↑↓ 1e
-25.21	-25.25	-26.05	-26.72	-27.52	↑↓ 1a ₁

^aSee Figure 13 for notation.**Figure 13.** Notation of assignments of orbitals in Table 18.

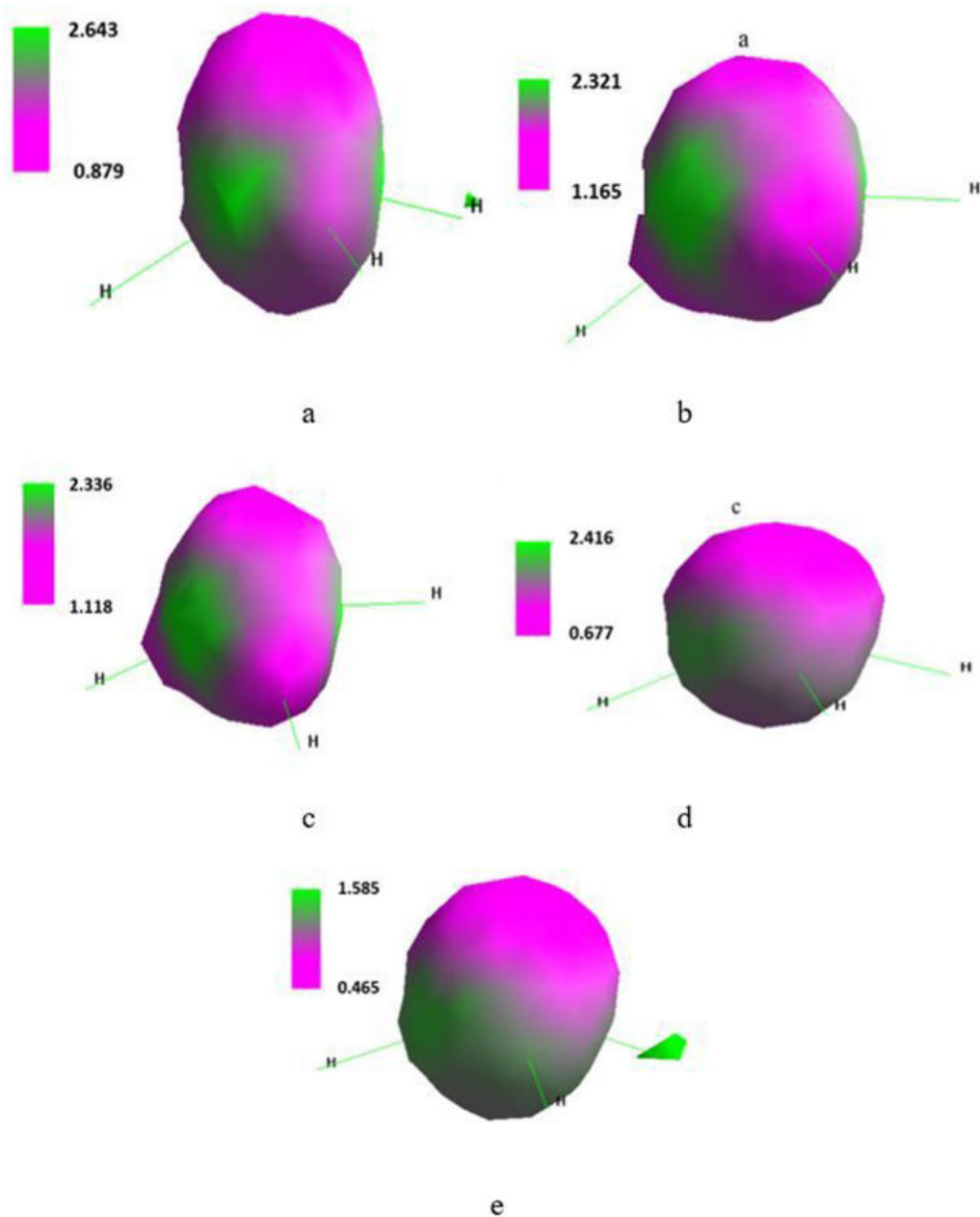


Figure 14. Isosurface along the x-axis of the Cartesian system of the single molecule of ammonia placed in SMF flux density of 0T (a), 0.1T (b), 1T (c), 10T (d) and 100T (e).

Table 19. Total, LUMO and HOMO energy of the system composed of three molecules of NH_3 placed in SMF flux density of 0 to 100T.

Parameter	Energy [kcal/mole] at flux density [T]				
	0	0.1	1	10	100
Total	235.4	236.5	254.5	278.6	296.8
LUMO	5.47	5.45	5.21	4.88	3.99
HOMO	-2.33	-2.17	-2.03	-1.92	-1.98
$\Delta_{\text{HOMO/LUMO}}$	7.80	7.64	7.24	6.80	5.97

Table 20. Maximal positive and negative charge density distribution in the system of three NH_3 molecules placed in SMF of the flux density of 0 to 100T.

Charge	Maximal charge density at flux density [T]				
	0	0.1	1.0	10	100
Positive	3.616	2.317	2.293	3.009	3.341
Negative	0.370	0.425	0.492	0.596	0.467

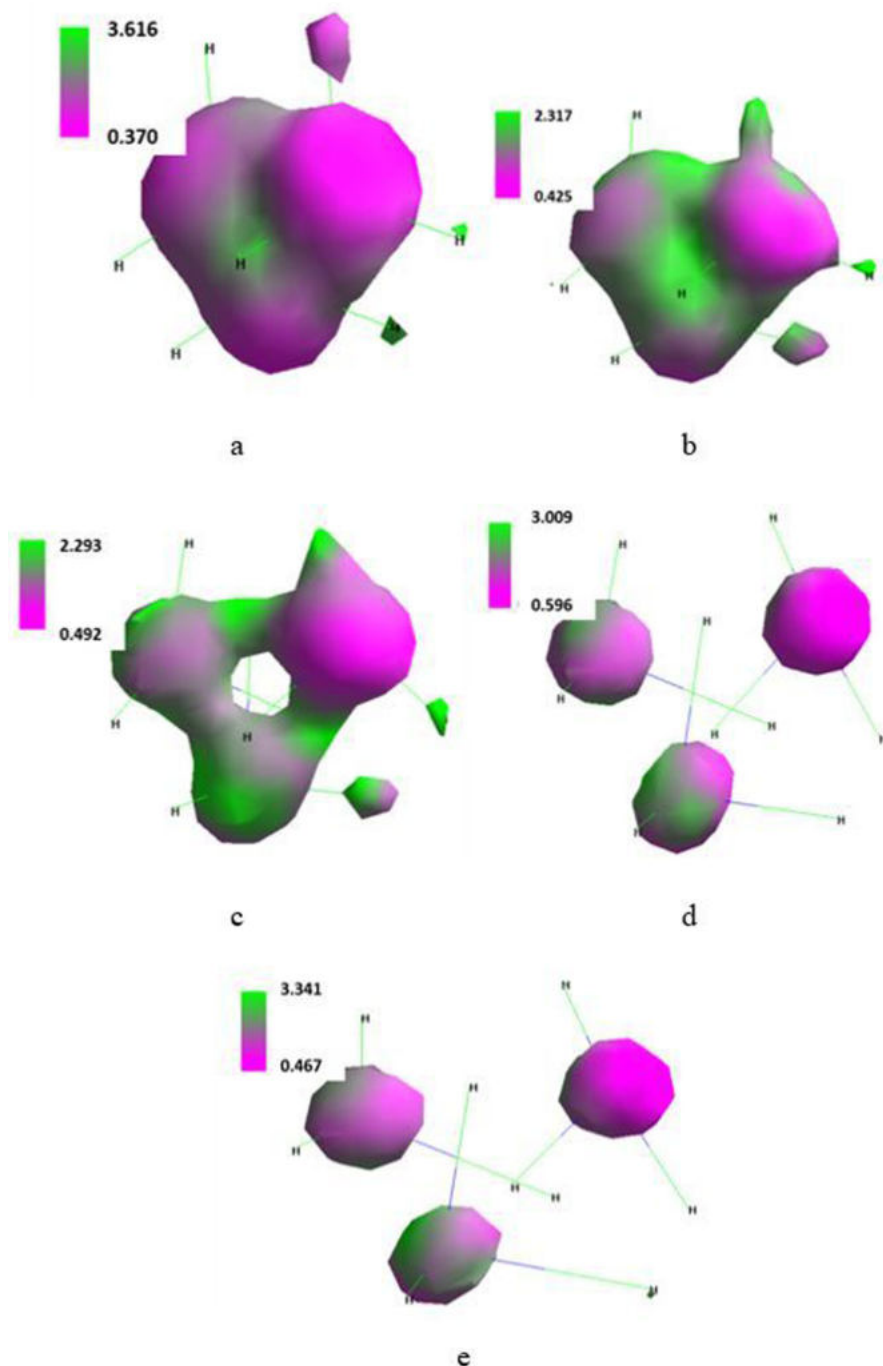
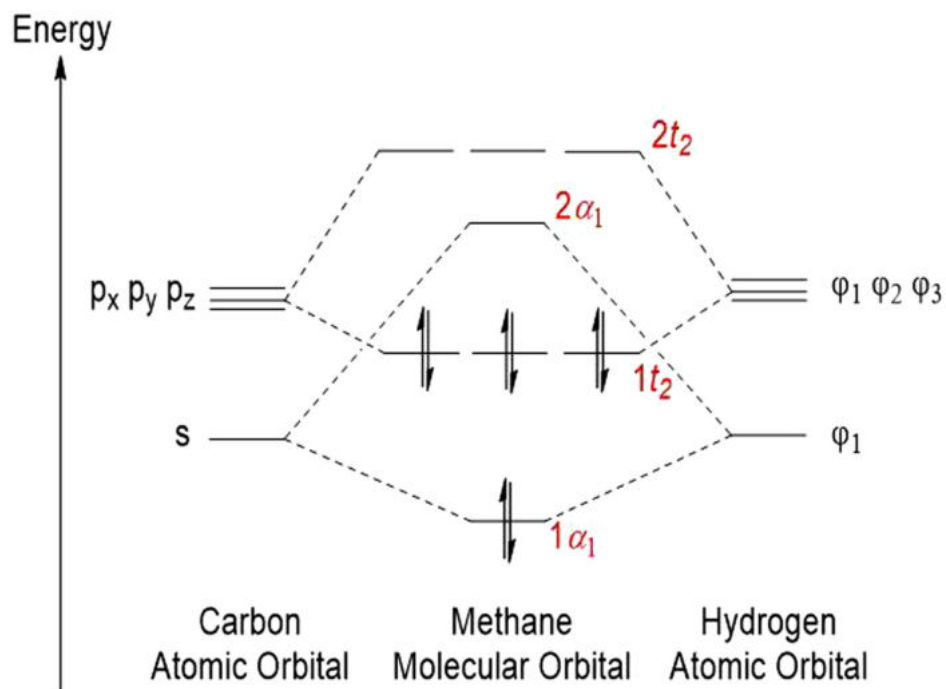


Figure 15. Isosurface along the x-axis of the Cartesian system of three molecules of ammonia placed in SMF of the flux density of 0T (a), 0.1T (b), 1T (c), 10T (d) and 100T (e).

Table 21. Properties of the single molecule of methane situated along the x-axis of the Cartesian system in SMF flux density of 0 to 100T.

Property		Flux density [T]				
		0	0.1	1	10	100
Maximal charge density	Positive	3.432	3.620	13.328	4.615	6.674
	Negative	2.458	2.523	1.946	2.050	3.314
Bond length [Å]	C-H1	1.0932	1.0932	1.0932	1.0938	1.0941
	C-H2	1.0932	1.0932	1.0932	1.0936	1.0941
	C-H3	1.0932	1.0932	1.0932	1.0936	1.0940
	C-H4	1.0932	1.0932	1.0932	1.0938	1.0939
Dipole moment [D]		0	0	0.001	0.001	0.001
Heat of formation [kcal/mole]		-70.8	-70.1	-69.4	-67.2	-62.3
Bond energy [kcal/mole]		413.2	413.2	412.8	411.9	411.3
Energy [kcal/mole] LUMO		9.76	9.76	9.78	9.78	10.81
HOMO		-15.02	-15.13	-15.18	-15.21	-16.34
Δ HOMO/LUMO [kcal/mole]		24.78	24.89	24.96	24.99	27.15

**Figure 16.** Notation of assignments of orbitals in Table 22.

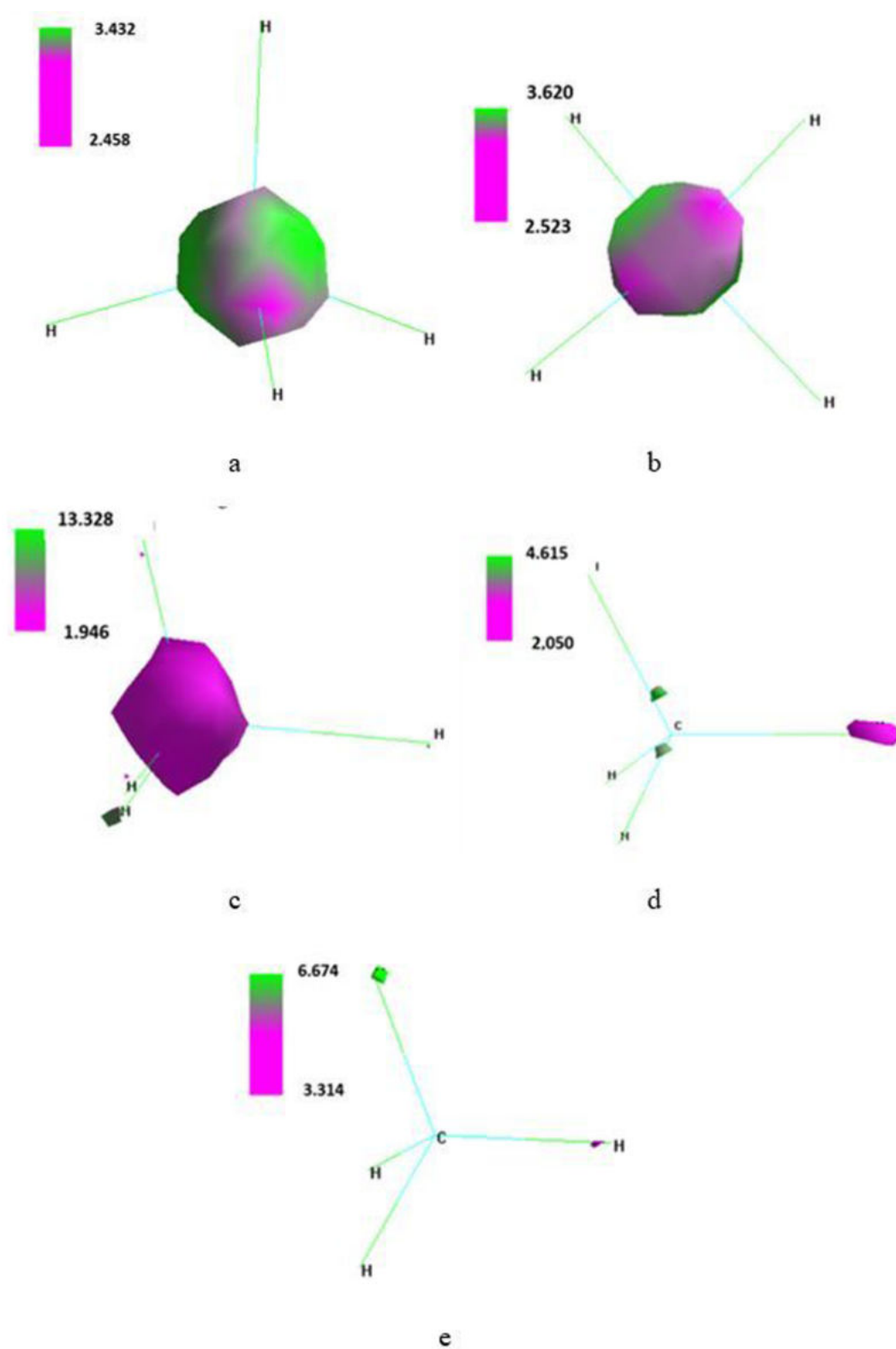


Figure 17. Isosurface along the x-axis of the Cartesian system of the single molecule of methane placed in SMF flux density of 0T (a), 0.1T (b), 1T (c), 10T (d) and 100T (e).

Table 22. Energy of electrons situated on particular orbitals in the single molecule of methane placed in SMF of the flux density of 0 to 100T.

Energy [kcal/mole] at flux density [T]					Orbital ^a
0	0.1	1.0	10	100	
9.76	9.76	9.78	9.78	10.81	3a ₁
-15.02	-15.13	-15.18	-15.21	-16.31	↑↓ 1b ₁
-15.02	-15.14	-15.19	-15.23	-15.32	↑↓ 2a ₁
-15.02	-15.13	-15.13	-15.22	-15.30	↑↓ 1b ₂
-16.72	-16.73	-17.31	-17.36	-17.39	↑↓ 1a ₁

^aSee Figure 16 for notation.

Table 23. Total, LUMO and HOMO energy of the system composed of three molecules of methane placed in SFM of the flux density of 0 to 100T.

Parameter	Energy [kcal/mole] at flux density [T]				
	0	0.1	1	10	100
Total	213.5	213.2	212.8	212.3	203.5
LUMO	9.05	9.11	10.21	11.23	12.85
HOMO	-1.48	-1.58	-1.83	-2.22	-3.22
$\Delta_{\text{HOMO/LUMO}}$	10.53	10.69	12.04	13.45	16.07

Table 24. Maximum of the positive and negative charge density distribution in the system of three methane molecules placed in SMF flux density of 0 to 100T.

Charge	Maximal charge density at flux density [T]				
	0	0.1	1.0	10	100
Positive	3.009	3.473	5.703	6.504	5.149
Negative	0.535	0.538	-2.988	-2.417	0.839

its first unoccupied orbital. Its energy expressed the energy required for the excitation of the methane molecule.

Pecularity mentioned above was rationalized in terms of the shape of isosurface of the molecule in particular values of flux density (Figure 17). At 1T, positive charge density concentrated almost completely on the carbon atom and its traces could be observed on two of four hydrogen atoms. The total positive charge density resided solely at one hydrogen atom. Increase in the applied T shifted the negative charge density completely to one of four hydrogen atoms. At 100T

only one hydrogen atom carried the negative charge density and another one held the positive charge density.

Total energy of the system built of three methane molecules slightly decreased when placed in SMF and a more considerable decrease was noted just at 100T (Table 23). Energy of LUMO and HOMO gradually increased and decreased, respectively. Maximal positive and negative charge density changed irregularly with increase in applied T (Table 24). Value of the $\Delta_{\text{HOMO/LUMO}}$ energy increasing with the SMF flux density pointed to reduced affinity of the system to the excitation.

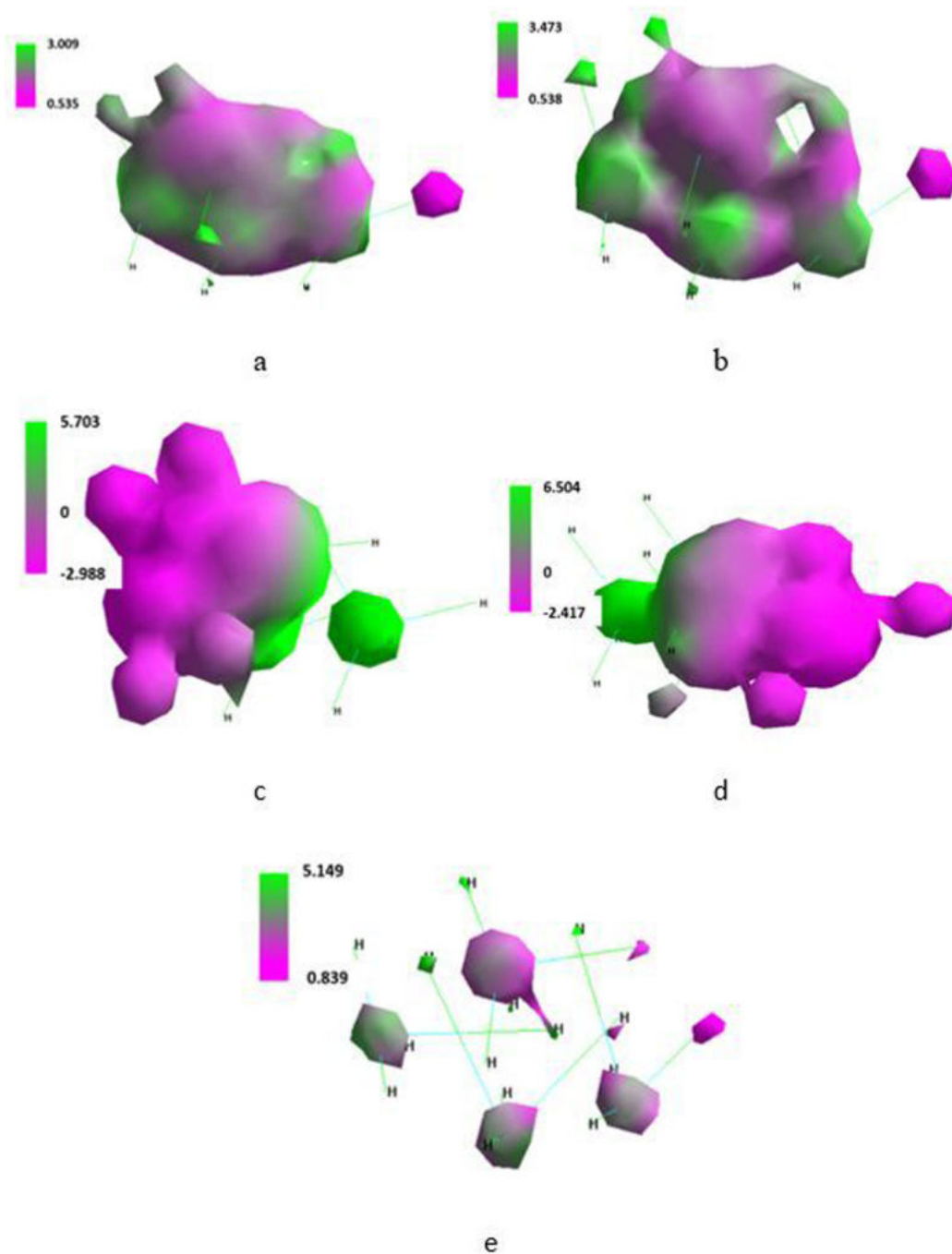


Figure 18. Isosurface along the x-axis of the Cartesian system of three molecules of methane placed in SMF flux density of 0T (a), 0.1T (b), 1T (c), 10T (d) and 100T (e).

Involving polar and van der Waals forces three molecules of methane formed various condensed structures. At 100T the system spread into three separate molecules (Figure 18).

Conclusions

Performed numerical simulations delivered strong evidence that small inorganic molecules commonly present in the

living organisms of flora and fauna can substantially influence functioning of those organisms residing in SMF.

Static magnetic field polarizes molecules of oxygen, nitrogen, water, ammonia, carbon dioxide and methane depending on applied flux density. Static magnetic field of up to 100T causes neither ionization nor breaking valence bonds of molecules placed in that field. In modelled computer vacuum three-molecular conglomerates of very dense packing form systems involving supramolecular orbitals.

Static magnetic field deteriorates supramolecular orbitals of three-molecular conglomerates developing highly polarized structures.

Static magnetic field reduces affinity of the molecules and their conglomerates to the excitation.

Data availability

All data underlying the results are available as part of the article and no additional source data are required

References

- Ueno S: **Biological Effects of Magnetic and Electromagnetic Fields**. New York: Plenum Press, 1993.
[Reference Source](#)
- Carpenter DO, Ayrappetyan S: **Biological Effects of Electric and Magnetic Fields**. Beneficial and Harmful Effects. New York: Academic Press, 1994; **2**.
[Publisher Full Text](#)
- Zhang X, Yarema K, Xu A: **Biological Effects of Static Magnetic Fields**. Singapore: Springer Nature, 2017.
[Publisher Full Text](#)
- Kirschvink JL, Kobayashi-Kirschvink A, Diaz-Ricci JC, et al.: **Magnetite in human tissues: A mechanism for the biological effects of weak ELF magnetic fields**. *Bioelectromagnetics*. 1992; **Suppl 1**: 101–113.
[PubMed Abstract](#) | [Publisher Full Text](#)
- Zannella S: **Biological effects of magnetic fields**. In: *CAS - CERN Accelerator School: Measurement and Alignment of Accelerator and Detector Magnets*. 1998; 375–86.
[Publisher Full Text](#)
- Anderson LE: **Biological effects of magnetic fields: laboratory studies**. *Proc. 20th Annu. Int. Conf. IEEE Engineering in Medicine and Biology Society. Biomedical Engineering Towards the Year 2000 and Beyond (Cat. No. 98CH36286)*. Hong Kong, China, 1998; **20**: 2791–2797.
[Publisher Full Text](#)
- Sabo J, Mirossay L, Horovcak L, et al.: **Effects of static magnetic field on human leukemic cell line HL-60**. *Bioelectrochemistry*. 2002; **56**(1–2): 227–231.
[PubMed Abstract](#) | [Publisher Full Text](#)
- Belyavskaya NA: **Biological effects due to weak magnetic field on plants**. *Adv Space Res*. 2004; **34**(7): 1566–1574.
[PubMed Abstract](#) | [Publisher Full Text](#)
- Formica D, Silvestri S: **Biological effects of exposure to magnetic resonance imaging: an overview**. *Biomed Eng Online*. 2004; **3**: 11.
[PubMed Abstract](#) | [Publisher Full Text](#) | [Free Full Text](#)
- Crozier S, Liu F: **Numerical evaluation of the fields induced by body motion in or near high-field MRI scanners**. *Progr Biophys Mol Biol*. 2005; **87**(2–3): 267–278.
[PubMed Abstract](#) | [Publisher Full Text](#)
- Ghodbane S, Lahib A, Sakly M, et al.: **Bioeffects of static magnetic fields: oxidative stress, genotoxic effects, and cancer studies**. *Biomed Res Int*. 2013; **2013**: 602987.
[PubMed Abstract](#) | [Publisher Full Text](#) | [Free Full Text](#)
- Driessen S, Bodewein L, Dechent D, et al.: **Biological and health-related effects of weak static magnetic fields (≤ 1 mT) in humans and vertebrates: A systematic review**. *PLoS One*. 2020; **15**(6): e0230038.
[PubMed Abstract](#) | [Publisher Full Text](#) | [Free Full Text](#)
- Hore PJ: **Upper bound on the biological effects of 50/60 Hz magnetic fields mediated by radical pairs**. *eLife*. 2019; **8**: e44179.
[PubMed Abstract](#) | [Publisher Full Text](#) | [Free Full Text](#)
- Ghadimi-Moghadam A, Mortazavi SMJ, Hosseini-Moghadam A, et al.: **Does exposure to static magnetic fields generated by magnetic resonance imaging scanners raise safety problems for personnel?** *J Biomed Phys Eng*. 2018; **8**(3): 333–336.
[PubMed Abstract](#) | [Free Full Text](#)
- Frankel J, Wilén J, Mild KH: **Assessing exposures to magnetic resonance imaging's complex mixture of magnetic fields for *in vivo*, *in vitro*, and epidemiologic studies of health effects for staff and patients**. *Front Public Health*. 2018; **6**: 66.
[PubMed Abstract](#) | [Publisher Full Text](#) | [Free Full Text](#)
- Mohajer JK, Nisbet A, Velliou E, et al.: **Biological effects of static magnetic field exposure in the context of MR-guided radiotherapy**. *Br J Radiol*. 2019; **92**(1094): 20180484.
[PubMed Abstract](#) | [Publisher Full Text](#) | [Free Full Text](#)
- Tenforde TS: **Interaction mechanisms and biological effects of static magnetic fields**. *Jpn Seminar on electromagnetic fields effects*. Sapporo, Japan. US Department of Energy, Contract DE-AC06-76RLO 1830. 1994.
[Reference Source](#)
- Rosen AD: **Mechanism of action of moderate-intensity static magnetic fields on biological systems**. *Cell Biochem Biophys*. 2003; **39**(2): 163–173.
[PubMed Abstract](#) | [Publisher Full Text](#)
- Okano H: **Effects of static magnetic fields in biology: role of free radicals**. *Front Biosci*. 2008; **13**: 6106–6125.
[PubMed Abstract](#) | [Publisher Full Text](#)
- Hernando A, Galvez F, García MA, et al.: **Effects of Moderate Static Magnetic Field on Neural Systems Is a Non-invasive Mechanical Stimulation of the Brain Possible Theoretically?** *Front Neurosci*. 2020; **14**: 419.
[PubMed Abstract](#) | [Publisher Full Text](#) | [Free Full Text](#)
- Hamza ASHA, Mohmoud SA, Ghania SM: **Environmental pollution by magnetic field associated with power transmission lines**. *Energy Conv Manag*. 2002; **43**(17): 2442–2452.
[Publisher Full Text](#)
- Ranković V, Ranković J: **Environmental pollution by magnetic field around power lines**. *Int J Qual Res*. 2009; **3**(3): 1–6.
[Reference Source](#)
- Committee to Assess the Current Status and Future Direction of High Magnetic Field Science in the United States, Board on Physics and Astronomy, Division on Engineering and Physical Sciences: **High Magnetic Field Science and Its Application in the United States: Current Status and Future Directions**. National Research Council, National Academy, Washington, D.C.: The National Academies Press, 2013.
[Publisher Full Text](#)
- Tang Y, Guo W, Lvov VS, et al.: **Eulerian and Lagrangian second-order statistics of superfluid ^4He grid turbulence**. *Phys Rev B*. 2021; **103**: 144506.
[Publisher Full Text](#)
- Bao S, Guo W: **Transient heat transfer of superfluid ^4He in nonhomogeneous geometries: Second sound, rarefaction, and thermal layer**. *Phys Rev B*. 2021; **103**: 134510.
[Publisher Full Text](#)
- Jaworska M, Domański J, Tomasiak P, et al.: **Preliminary studies on stimulation of entomopathogenic nematodes with magnetic field**. *Prom Zdr Ekol*. 2017; **4**: #9.
- Jaworska M, Domański J, Tomasiak P, et al.: **Methods of stimulation of growth and pathogenicity of entomopathogenic fungi for biological plant protection**. *Polish Patent*. 2014; 223–412.
- Jaworska M, Domański J, Tomasiak P, et al.: **Preliminary studies on stimulation of entomopathogenic fungi with magnetic field**. *J Plant Dis Protect*. 2016; **12**: 295–300.
- Białopiotrowicz T, Ciesielski W, Domański J, et al.: **Structure and physicochemical properties of water treated with low-temperature low-frequency plasma**. *Curr Phys Chem*. 2016; **6**(4): 312–320.
[Publisher Full Text](#)
- Ramya KR, Venkatnathan A: **Density functional theory study of oxygen clathrate hydrates**. *Indian J Chem*. 2013; **52A**: 1063–1065.
[Reference Source](#)
- Marchand N, Lienard P, Siehl HU, et al.: **Applications of molecular simulation software SCIGRESS in industry and university**. *Fujitsu Sci Technol J*. 2014; **50**(3): 46–51.
[Reference Source](#)
- Frisch MJ, Trucks GW, Schlegel HB, et al.: **Gaussian 09, Revision A.02**.

Wallingford CT: Gaussian, Inc., 2016.

[Reference Source](#)

33. Farberovich OV, Mazalova VL: **Ultrafast quantum spin-state switching in the Co-tetraethylporphyrin molecular magnet with a terahertz pulsed magnetic field.** *J Magnet Magnet Mater.* 2016; **405**: 169–173.
[Publisher Full Text](#)
34. Charistos ND, Muñoz-Castro A: **Double aromaticity of the B-40 fullerene: induced magnetic field analysis of pi and sigma delocalization in the boron cavernous structure.** *Phys Chem Chem Phys.* 2019; **21**(36): 20232–20238.
[Publisher Full Text](#)
35. Glendening ED, Reed AE, Carpenter JE, et al.: **Extension of Lewis structure concepts to open-shell and excited-state molecular species, NBO Version 3.1.** *PhD thesis.* University of Wisconsin, Madison, WI. 1987.
36. Carpenter JE, Weinhold F: **Analysis of the geometry of the hydroxymethyl radical by the “different hybrids for different spins” natural bond orbital procedure.** *J Mol Struct (Theochem).* 1988; **169**: 41–62.
[Publisher Full Text](#)
37. Froimowitz M: **HyperChem: a software package for computational chemistry and molecular modeling.** *Biotechniques.* 1993; **14**(6): 1010–1013.
[PubMed Abstract](#)
38. Wayne RP: **Singlet molecular oxygen.** *Adv Photochem.* 1969; **7**: 311–371.
[Publisher Full Text](#)
39. Schweitzer C, Schmidt R: **Physical mechanisms of generation and deactivation of singlet oxygen.** *Chem Rev.* 2003; **103**(5): 1685–1757.
[PubMed Abstract](#) | [Publisher Full Text](#)
40. Ruscic B, Pinzon RE, Morton ML, et al.: **Introduction to active thermochemical tables: Several “key” enthalpies of formation revisited.** *J Phys Chem A.* 2004; **108**(45): 9979–9997.
[Publisher Full Text](#)
41. Golde MF, Trush BA: **Formation of excited states of N₂ from ground state nitrogen atoms.** *Faraday Disc Chem Soc.* 1972; **53**: 52–62.
[Publisher Full Text](#)
42. Kirillov AS: **Electronically excited molecular nitrogen and molecular oxygen in the high-latitude upper atmosphere.** *Ann Geophys.* 2008; **26**: 1159–1169.
[Publisher Full Text](#)
43. Franks F: **Water: a Matrix for Life.** (2nd Ed.). Royal Society of Chemistry. London, 2007.
44. Ma Y, Peng L, Zhang H, et al.: **The potential energy surfaces of the ground and excited states of carbon dioxide molecule.** *Rus J Phys Chem.* 2014; **88**: 2339–2347.
[Publisher Full Text](#)
45. Bultel A, Schneider IF, Babou Y: **CO and C₂ excited states relaxation in CO₂ plasmas derived from a Collisional-Radiative model.** *J Phys Conf Ser.* 15th Int Congr Plasma Phys (ICPP2010) & 13th Latin American Workshop Plasma Phys, (LAWPP2010) 8–13 August 2010, Santiago, Chile. 2010; 511.
[Publisher Full Text](#)
46. Gil GS: **Excited states of ammonia and the Jahn-Teller effect ab initio and force field calculations.** *MSc Final Project.* University of Bristol, UK. 2015.
[Reference Source](#)
47. Montagnani R, Riani P, Salvetti O: **Ab initio calculation of some low-lying electronic excited states of methane.** *Theor Chim Acta.* 1973; **32**: 161–170.
[Publisher Full Text](#)

The benefits of publishing with F1000Research:

- Your article is published within days, with no editorial bias
- You can publish traditional articles, null/negative results, case reports, data notes and more
- The peer review process is transparent and collaborative
- Your article is indexed in PubMed after passing peer review
- Dedicated customer support at every stage

For pre-submission enquiries, contact research@f1000.com

F1000Research